Heliyon 10 (2024) e32717

Contents lists available at ScienceDirect

Heliyon

journal homepage: www.cell.com/heliyon

Research article

Bioassay-guided fractionation of *Verbascum thapsus* extract and its combination with polyvinyl alcohol in the form electrospun nanofibrous membrane for efficient wound dressing application

Sepideh Razani [a], Mohsen Farhadpour [b], Manizheh Avatefi Hemmat [a], Fatemeh Sadat Alamdaran [a], Masoumeh Fakhr Taha [c], Hossein Ali Khonakdar [d], Matin Mahmoudifard [a,*]

[a] *Department of Industrial and Environmental Biotechnology, National Institute of Genetic Engineering and Biotechnology (NIGEB), Tehran, Iran*
[b] *Department of Plant Bioproducts, National Institute of Genetic Engineering and Biotechnology (NIGEB), Tehran, Iran*
[c] *Department of Stem Cells and Regenerative Medicine, Institute for Medical Biotechnology, National Institute of Genetic Engineering and Biotechnology, Tehran, Iran*
[d] *Department of Polymer Processing, Iran Polymer and Petrochemical Institute, Tehran 14965-115, Iran*

ARTICLE INFO

Keywords:
Verbascum thapsus
Nanofibers
Nanotechnology
Wound healing
Excisional wound

ABSTRACT

Verbascum thapsus (*V. thpsus*), family Scrophulariaceae, has considerable importance in traditional medicine worldwide because of its antioxidant and anti-inflammatory activities. *V. thpsus* was used in traditional medicines as a useful drug for lung disease, sore throat, wound healing, and treatment of whooping cough. The aim of this study was to extract of *V. thpsus* bioactive fraction using antibacterial assay guided fractionation methodology and develop a system based on electrospun nanofibrous membrane (NFM) that can be effective by releasing the extract of *V. thapsus* for antibacterial and wound healing applications. For this purpose, the fractionation of total extract was done using Liquid-Liquid extraction method. The selected fraction based on its anti-bacterial activity was then subjected to the silica gel column chromatography for further purification. Since electrospinning is an economical and relatively simple method to produce continuous and uniform nanofibers, and due to its high specific surface area, adjustable pore size, and flexibility, special attention has been paid to loaded the most effective fraction on PVA nanofibers for applications such as wound dressings. The obtained result showed that, the purified *V. Thapsus* extract has a concentration-dependent antimicrobial activity against *Escherichia coli* and *Staphylococcus aureus*. The phytochemically analyses of bioactive fraction by High-performance liquid chromatography (HPLC) proved the presence of 6 phenolic acids, 4-hydroxybenzoic acid, chlorogenic acid, caffeic acid, *p*-coumaric acid, ferulic acid, and flavonoid, rutin, as the major compounds. Also, physicochemical characterization of PVA-selected extract loaded electrospun nanofibrous membranes (NFM) were analyzed by scanning electron microscope (SEM), Fourier transform infrared spectrometer (FT-IR). MTT and hemolysis assays were done to affirm the biocompatibility of fabricated scaffolds. Release profile of extract loaded- NFM showed continues release of extract from mat during 90h. Moreover, the capability of these NFM in wound healing application was evaluated in-vitro and in-vivo. The cell viability test (MTT), cell adhesion images, antioxidant, antibacterial, hemolysis assays and in-vitro and in-vivo wound healing assays confirmed that fabricated NFM containing 5 % butanolic extract were the most

* Corresponding author.
E-mail addresses: m_mahmodifard@nigeb.ac.ir, matinmahmodifard@yahoo.com (M. Mahmoudifard).

https://doi.org/10.1016/j.heliyon.2024.e32717
Received 20 February 2024; Received in revised form 6 June 2024; Accepted 7 June 2024
Available online 7 June 2024

biocompatible scaffold for wound dressing applications and accelerates the rate of wound closure. The obtained outcomes confirmed that *V. thpsus/PVA* NFM can be considered as promising scaffold for potential wound dressings.

1. Introduction

Wounds are physical injuries that cause opening or tearing of the skin, which can lead to anatomical and functional disorders. Skin wounds cause the connection between the epithelium and the underlying connective tissue to be lost [1]. Wound healing is a complex process that restores tissue integrity and homeostasis and includes four stages. These stages include homeostasis, inflammation, proliferation, and tissue regeneration. Many factors can affect wound healing, but generally, this process is mediated by a complex signaling mechanism involving various growth factors, cytokines, and chemokines [2]. The proliferation and migration of epidermal cells is an essential repair process in wound healing. The cells of the epidermis at the edges of the wound undergo structural alterations that allow them to detach from their attachments to other epidermal cells and their basement membrane [3]. Using plants and herbal medicines in treating patients has remained an old method due to their extraordinary effect. A significant percentage of drugs are extracted from different plants with many potential properties [4]. Many phytochemical substances, such as phenols, terpenoids, and alkaloids in plants, have antimicrobial and antioxidant properties [5].

V. thapsus as the species of Scrophulariaceae plant family is an annual or biennial shrub and is distributed worldwide and grows in Asia, North Africa, North America, and Europe [6]. Dry powder and poultice of its leaves are usually used for severe wounds of any kind. It has been reported it has no side effects and has therapeutic properties in lung disease, sore throat, wound healing, and treatment of whooping cough [7]. In the homeopathic treatment methods, various formulations of *V. thapsus* have been used to cure burn and earache wound and tumors. Some other formulations can also be used for the treatment of long-term headaches, oxidation inhibitors, reduction of body odor and skin aging [8]. Also, the hydroalcoholic *V.thapsus* extract has shown a healing effect on the skin wound and the regeneration of the epidermis layer at the wound site [6]. Khan et al. reported the antibacterial activity of methanolic extract of *V. thapsus* shoot against gram positive and gram negative with favorable MIC value [9]. Antiviral activity study of *V. thapsus* extract showed the strong antiviral activity against influenza virus with IC50 < 6.25 mgmL^{-1} [10]. In the study of Taleb et al., the cream prepared from *Verbascum* plant extract showed a significant effect on episiotomy pain in 100 primiparous women [11].

On the other hand, nanotechnology is an innovative and vital technology with many applications in various fields like energy, environment, medicine, and drug delivery [12]. Nanotechnology is related to systems and materials that exhibit new and improved chemical, physical, and biological properties, processes, and phenomena due to their nanoscale size and structure. The definition of nanotechnology is "the design, characterization, fabrication, and controlled application of the shape and size of materials at the nanoscale" [13–15].

It has been stated that polymeric nanofibrous membranes have broad applications in nanotechnology. Nanofibers can be produced using a simple, versatile, and widely used method called electrospinning [16]. Currently, electrospun polymer nanofibers are widely used in different fields including tissue engineering, drug delivery, biosensors, filtration, batteries, and so on [17–20]. Their importance is due to the unique properties of them such as high surface area and porosity, electrical, chemical and mechanical, properties. There are different techniques for the synthesis of nanofibers. Which among them electrospinning is the most favorite technique used for widely for the synthesis of nanofibers with different morphologies [21–23].

Electrospinning enables the fabrication of scaffolds that can be modified both during the electrospinning process and after fabrication to be used for specific biomedical applications. The selected polymer plays an essential role in the level of drug release from the nanofiber structure, which determines the rate of degradation and releases through the scaffold [24]. The structure of nanofibers modulates the interaction of the dressing surface with blood cells and damaged tissue. Also, the layered structure of nanofiber gives it good elasticity and proper liquid absorption, and by increasing the speed of absorption, it creates a suitable environment for treating deep wounds [25].

Recently, these nanofibers have been used for dressing skin wounds due to their characteristics, such as porosity and their similarity with the natural extracellular matrix tissue in the skin. They have the ability to strengthen the wound healing process [26]. The selection of scaffold ingredients has an influential role in the success of skin tissue engineering and wound dressing. Different natural and synthetic materials are used to make these biomedical scaffolds. In comparing natural and synthetic types, it has been proven that,the synthetic polymers have better mechanical properties than natural polymers and are easy to process but show less biological activity [27]. Therefore, it seems that the combination of synthetic and natural components for the generation of ideal scaffold for biomedical applications is the most feasible approach. In this regards, here, in the first step, we have obtained *aqueous*, *ethyl acetate* and *butanolic* extracts of *V. thapsus* and test their antibacterial properties through MIC and MBC assays and selected the best one for the next step of NFM fabrication. Then, PVA NFM with various concentrations of *V. thapsus butanolic* extract, the most effective extract obtained, was prepared and tested for its ability in wound healing using different approaches.

2. Material and method

2.1. Plant materials

The aerial parts of flowering *V. thapsus* were gathered on the outskirts of Sari, Mazandaran province, located in northern of Iran,

and confirmed by the National Institute of Genetic Engineering and Biotechnology (Tehran, Iran) laboratory. Following the collection, the plant material underwent a cleaning process, and was then dried for 72 h at a temperature of 40 °C in a well-ventilated oven.

2.2. Extraction and purification of V. Thapsus plant

About 50 g of dried arial part of *V. thapsus* plant was powdered and macerated in 80 % Ethanol (1:10, w/v), for overnight. The extracts were filtered and this procedure was repeated two times. The solvent was evaporated at 40 °C by a rotary evaporator to produce a dry extract. 50 mg of the extract was dissolved in water and partitioned with EtOAc using Liquid-Liquid extraction procedure. The EtOAc portion was dried and loaded on to column chromatography over a Silica gel (60–120 mesh) eluting with 200 mL of 90:10, 80:20, 50:50, 10:90 and 0:100 (v:v) of Hexan - EtOAc. In the next step, 50 ml of the extract obtained from the dried VT plant was dissolved in 300 ml of distilled water, and 300 ml of butanol was added. The solution was transferred to the separation funnel to be saturated and separated. In total, three fractions were obtained from the *V. thapsus* extract, which were separated by *ethyl acetate*, *water*, and *butanol*, then lyophilized and dried. Finally, the obtained fractions were concentrated and subjected to their antibacterial activity assay.

2.3. HPLC analysis

All chemicals and reagents used for analyses of total phenolic compounds were purchased from Sigma–Aldrich (Deisenhofen, Germany). The HPLC grade methanol, water and trifluoroacetic acid were obtained from Merck (Darmstadt, Germany). The phenolic compound standards; Gallic acid, 4-hydroxy benzoic acid, chlorogenic acid, caffeic acid, cinnamic acid, quercetin and rutin were also purchased from Sigma–Aldrich (Deisenhofen, Germany). Quantification of phenolic acids and flavonoids in extracts were done by use of Agilent 1260 Infinity HPLC system (USA) equipped with a solvent delivery quaternary pump, degasser, an auto-sampler, and Photo Diode Array detector. The chemstation software was used for recording the chromatogram. The zorbax C18 column with dimensions of 4.6 mm * 250 mm, 5 μm 100 ^{o}A, was used for phenolic analyses at 20 °C (USA). The mobile phase consisted of Solvent A (H_2O + 0.02 % trifluoroacetic acid) and solvent B (MeOH + 0.02 % TFA) was applied. The best separation was achieved using a flow rate of 0.7 mL min^{-1} of the following gradient elution: 0–5 min, 5 % solvent B, which increases to 15 % in 15 min; 15–25 min, 35 % solvent B; 25–45 min, 55 % solvent B, and 45–55 min, 100 % solvent B. For the study of phenolic compounds, chromatograms were obtained at 218 nm, 254 nm, 270 nm, and 305 nm. The samples were identified using available standards, retention times, and UV spectra. The peak area was used to quantify the detected chemicals.

2.4. Preparation of PVA/VT electrospun nanofibrous membranes

Poly (vinyl alcohol) (PVA, MW = 72,000 g/mol; 86 % hydrolyzed) was obtained from Sigma-Aldrich. The Butanolic extract of VT (2, 5, 10 w/v) were dispersed in PVA solution (10 %, w/v) with continuous stirring for 6 h, at 70 °C in a sealed vial to obtain a uniform solution. The solution was then poured into four 5 ml syringes and was placed into pumps. An electrospinning setup with four syringe nozzles was employed to produce the nanofibers. An aluminum foil was wrapped around a rotating drum with a needle tip to a collector distance of 15 cm to obtain a uniform nanofibrous membrane. The experiment was carried out in a room with a relative humidity of 65 % and a temperature of 27 °C. The applied voltage between the needle and collector was set at 16 kV, and the optimal distance was determined to be 15 cm. the speed of rotating collector was adjusted to 500 rpm and the Debi of injecting pumps were set as 0.5 ml/h. In order to get water stable NFM, as synthetized membranes were cross-linked by putting them in a sealed desiccator where a plate of glutaraldehyde and hydrochloric acid with the 9:1 v/v ratio was place in the bottom of it (for 6 h at a temperature of 40 °C). Then the obtained scaffolds were placed in a vacuum oven for 24 h to remove the residue of glutaraldehyde. The morphology characteristic of the obtained NFM was assayed by scanning electron microscopy (SEM; Philips XL30, Netherlands). For this purpose, a small piece of each sample was gold sputter coated, and then placed on the sample holder and an acceleration voltage of 10 kV was used to obtain SEM images. Furthermore, the chemical nature of NFMs was studied by FTIR technique (Bruker Vertex 70, Germany), at wavenumbers ranging between 400 and 4000 cm−1.

2.5. Characterization

2.5.1. In vitro drug release study

An amount of 20 mg of the VT loaded NFMs were placed in 2 mL of PBS (pH: 7.4) in a test tube with a shaking of 180 rpm and a temperature of 37 °C. The solution was sampled at determined time intervals, and its absorbance was read at 675 nm (as specific absorbance peak for VT) using a spectrophotometer (model UV2401; Shimadzu, Japan) for 90 h. The same volume of PBS was added to the sample each time so that the total volume did not change. The absorptions obtained were analyzed with VT concentration/OD (optical density) standard curve and the cumulative released of samples were calculated using the following equation [28]. In order to obtain the total amount of VT in electrospun nanofibers 20 mg non-cross linked NFM were dissolved completely in DI and the absorbance was obtained in 675 nm and using calibration curve, the extract concentration was obtained.

$$Cumulative\ release\ (\%) = \frac{(VT\ amount\ in\ the\ release\ medium)}{(Total\ amount\ of\ laoded\ in\ the\ NFM\ )} \times 100$$

2.5.2. Evaluation of the membranes' porosity

The measurement of the nanofibrous scaffolds' porosity involved immersing the membrane in ethanol for 1 h, followed by an assessment of the quantity of solvent absorbed by the membrane. For this test, the scaffolds were cut with a 20 mm diameter punch and their dry weight was measured. Then they were immersed in ethanol for 1 h and the wet weight of scaffold was obtained right after expelling from ethanol. The estimation of the membrane's porosity was determined using the subsequent equation:

$$porosity(\%) = \frac{Ww - Wd}{Dethanol \times Vmembrane} \times 100$$

The weight of the wet membrane (W_w) and the weight of the dry membrane (W_d) were considered in the calculation. Additionally, the density of ethanol ($D_{ethanol}$) and the volume of the wet membrane ($V_{membrane}$) were taken into account [29].

2.5.3. Water vapor transmission rate

To this end, a glass tube with an area of 1.77 cm2, filled with 10 mL of pure water, that its opening covered by samples. The membrane was secured onto the glass tube opening using parafilm to prevent water loss. A tube without any cover and another one with complete cover using parafilm were used as controls. Subsequently, the tubes were left to incubate for a day at 37 °C, and the reduction in weight of the water in glass tube was measured to ascertain the extent of water evaporation. The water vapor transfer rate of the membranes was determined using the subsequent equation [30].

$$\text{Water Vapor Transmission Rate} = W_{loss}/A$$

Where *W*loss is the amount of weight loss of water, and *A* is the area of the tube opening.

2.5.4. Swelling and biodegradation studies

The swelling behavior of VT-PVA membranes was determined by immersing 20 mg of membranes in distilled water for 24 h at 25 °C. Subsequently, the samples were retrieved and reweighed. The extent of swelling was calculated by comparing the weights of membranes before and after the swelling process. The degradability of VT-PVA membranes was investigated in simulated body fluid (PBS, pH 7.4). A 20 mg sample of VT-PVA membrane was placed in 50 mL of media for 30 days at 37 °C. Following the incubation period, the membranes were retrieved, rinsed, dried and reweighed. The percentage of weight loss was determined by comparing the final weight of the membranes to the initial weight as a control [31].

2.5.5. Mechanical properties

The Shimadzu tensile tester (ASTM D256) was utilized to examine the mechanical characteristics of the scaffolds. Each scaffold (three samples in total) was precisely cut into rectangular dimensions measuring 20 × 10 mm, with thicknesses ranging from 0.22 to 0.31 mm [32].

2.5.6. Contact angle analysis

The contact angles of the PVA/VT composite nanofiber membranes were assessed through the utilization of a contact angle analyzer (DCAT 21, Dataphysics Instrument GmbH, Germany). Strips of electrospun nanofiber membranes, sized at 2 cm × 3 cm, were utilized, followed by the application of 2 μl of distilled water onto the surface of the nanofiber membranes. Subsequently, the contact angles of the droplets on the surface were gauged. This process was conducted in triplicate to validate the results [33].

2.6. Cell studies

2.6.1. Cell culture and seeding

L929 fibroblasts cell was obtained from cell bank of NIGEB and cultured in RPMI 1640 (Gibco,USA) containing 10 % FBS (Gibco, USA), 100 units/mL penicillin (P4333; Sigma), 100 mg/mL streptomycin (P4333; Sigma). Then, it was incubated at 37 °C and 95 % air and 5 % CO2 were served for all cell culturing and cell seeding process. The experiments were performed after three passages of cell and media was replaced three times in the week.

In order to cell culturing on NFM, Different types of scaffolds were punched and placed in 96-well plates. Then scaffolds were sterilized with a brief convenient method. Shortly, the scaffolds were immersed in 70 % ethanol for 30min under UV irradiation to sterilize them. Then they were washed thrice with PBS each 10min to remove ethanol from scaffold. After 2 h of equilibration of the scaffold with complete media, media was removed and cells were seeded on scaffolds.

2.6.2. Cellular adhesion and morphology evaluation

L929 cells morphologies on VT-loaded NFMs were visualized through SEM and DAPI staining at days 1 and 3 after cell seeding. For this purpose, the preparation of biological samples followed by fixing with glutaraldehyde solution (Sigma, 2.5 %) and dehydration treatment which then were treated with graded series of alcohol (30, 50, 60, 70, 80, 90, and in the end 100 %). After drying, the scaffolds were spattered with gold and analyzed through SEM (Philips XL30, Netherlands) to observe the morphologies of the cells on NFM at an accelerating voltage of 26 kV. On the other hand, cell adhesion was evaluated on the VT loaded NFM by DAPI staining. To this aim, after cell ceding on different NFM with different concentrations of the extract, cells were washed three times with PBS then being fixed with 4 % paraformaldehyde for 20 min at ambient condition. DAPI (2 μl/ml in PBS buffer, pH:7.4) was then used to stain

the cell nucleus for 15 min in dark place. After incubation, scaffolds were washed 5 times with PBS buffer to remove excess dye. Finally, cell morphology was observed under a fluorescence microscope. (Nikon, Eclipse TE2000-S, Japan)

2.6.3. Cell viability assay

MTT assay was carried out using a standard testing protocol [ISO10993–5:2009(E)] to determine the viability of cells on *VT loaded* NFM with different concentration of *butanolic* extract. Tetrazolium molecules of MTT were reduced by viable cells into colored formazan product that is a representation of the mitochondria normal activity. In this regard for determining the level of cellular metabolism, the level of the reduction of MTT into formazan was measured. For this purpose, L929 fibroblast cells were seeded on the samples with the density of 10000 cells in each well. The cell seeded sterilized scaffolds were kept at 37°Cunder 5 % CO_2 for 1, 3 and 7 days. After the incubation for aforementioned time, MTT solution (200 μL of 0.5mgmL^{-1}) was added to every well and the plate was incubated at 37 °C during 4 h. Finally, the solution was removed from each well, and 200 μL of DMSO was added to every well, shaked and incubated for 20 min to solubilize formazan crystals. Then, 100 μl of DMSO from each well was transferred to another well, and the solution absorbance was measured at 570 nm wavelength using an ELISA plate reader (Biorad, USA). The experiments were repeated in 5 times and the mean value was reported for each group.

2.6.4. Cell migration assay/in-vitro scratch wound assay

First of all, VT- NFM juices were prepared for all ratios. To this end, the scaffolds were punched in 1*1 cm^2 and put inside labeled micro tubes containing 500 μl PPMI medium (without FBS, without Penicillin and Streptomycin (Pen-Strep)) for 3 days. When L929 cells population was reached a confluence of 90 % in 25 cm2 flask, the cells were counted and 30000 cells seeded into each well of 48-well plate with complete RPMI medium (200 μL) and incubation under 5 % carbon dioxide, 37 °C condition for 24 h. Then, using a pipette tip, a scratch wound was created across the well. Subsequently, the cells were treated with 3 days prepared juices in which 180 μL juice added to cell-seeded plates with addition of 20 μL FBS, then plates kept under 5 % carbon dioxide, 37 °C condition for 24 h. On different hours after treatment, the area of wound was controlled through optical microscopy and imaged.

2.7. Hemolysis assay

Healthy human blood was used in this experiment. For this purpose, fresh blood was obtained in the medical diagnostic laboratory. 5 mL of fresh blood was added to the 10 ml 0.9 % saline solution and centrifuge at 500 g for 10 min in order to separate serum from RBCs. The above mentioned step was repeated 5 times to obtain pure RBC. In the last step, supernatant was discarded and the plat of RBCs was diluted in 50 ml PBS buffer (ph = 7.4) and used as stock solution. Electrospun sheets of PVA, PVA-E2%, PVA-E5% and PVA-E10 % were cut in the same dimensions (1 × 1 cm2) and incubated in 0.8 ml saline solution for 24 h, then 0.2 mL of stock blood solution was added to each tube and incubated for 30 min at 37 °C. For positive and negative control, PBS and DI water without electrospun nanofibers were considered as 0 %–100 % hemolysis sample. After the incubation time, the solution of each tube was centrifuged and the optical density (OD) of the supernatant solution was checked at a wavelength of 545 nm. Hemoglobin amount and hemolysis percentage were obtained using the following equation [28].

$$Hemolysis\ (\%) = \frac{(\mathrm{OD}\ \ of\ sample - OD\ of\ negative\ control)}{(OD\ of\ positive\ control - \ OD\ of\ negative\ control)} \times 100$$

2.8. Determination of the minimum inhibitory concentrations (MIC) and MBC

For this purpose, the bacteria were incubated for 16 h in Mueller Hinton culture medium at 37 °C. The prepared culture medium was used for MIC test and to check the antibacterial properties of the extract against *Escherichia coli (ATCC 25922)* and *Staphylococcus aureus (ATCC 25923)*. A certain amount of plant extract was weighed and after preparation of serial dilution, it was transferred to a flat-bottom 96-well microplate (SPL Life Sciences Co., Pocheon-si, South Korea). Each extract was tested at a concentration of 1.0, 0.5, 0.25 and 0.1 mgmL^{-1}. McFarland's bacteria were diluted to a concentration of 1*10^5. Then, to evaluate the inhibition of bacterial growth after 24 h, a measurement was done at OD of 600 nm. Tetracycline and chloramphenicol were used as standard positive controls and sample free solutions as blank controls. Each test was replicated three times.

2.9. Antibacterial properties

2.9.1. Evaluation of V. Thapsus by normal saline test (CFU, colony-forming unit)

In order to check the antibacterial properties of VT loaded NFMs, a colony count test was designed with normal saline method [34]. For this assay, briefly, 5 mg of sterilized nanofibers were weighted and placed to Erlenmeyer containing 4.5 ml of saline solution (0.9 % NaCl in DI) and then 0.5 ml of bacteria stock solution with a final dilution of 10*10^5 was added to each container and incubated at 37 °C with a shaker of 180 rpm for 4 h. Then, the diluted solution inside each Erlenmeyer flasks was cultured on a solid plate containing LB medium and incubated overnight at 37 °C. The number of colony appeared on the plates after incubation were counted and evaluated for determination of antibacterial efficiency of different NFM against *Escherichia coli (E. coli)* and *Staphylococcus aureus (S. aureus)* bacteria. In order to assess the morphology evolution of bacteria after encountering VT loaded NFM, the above mentioned saline solution was filtrated through 0.22 μm filter. Afterward, the glutaraldehyde 2.5 % was passed through this filter. The present glutaraldehyde in the filter remains in contact with the captured bacteria for 3 h. Afterward, the dehydration step with the ethanol

gradient was done with the filtering of 30, 50, 70, 90, and 100 % ethanol, respectively, and incubation of each one for 15 min. Then, the mesh of the filter had been extracted and scanning electron microscopy was done after the gold sputtering.

2.9.2. Disk diffusion method

The antibacterial test was conducted using the disc diffusion method on a sterile Mueller-Hinton agar culture medium. The required amount of bacteria was inoculated into the culture medium and incubated at 37 °C for 24 h 100 μL of 10^5 CFU per mL of bacterial suspension cells was inoculated onto nutrient agar plates. For inoculation, a sterile cotton swab was used and the bacteria were evenly spread on the entire plate's surface by swabbing in three different directions. Nanofibers contained different percent of the extract with a diameter of 10 mm were placed on the agar medium, and samples were then placed in a 37 °C incubator. After 24 h, the antibacterial activity of the samples was assessed. ImageJ software was utilized to calculate the radius of the zone of inhibition [35].

2.10. Determination of antioxidant activity (DPPH)

The antioxidant efficiency of the *butanolic* VT extract was evaluated by the method of scavenging the stable 1, 1-diphenyl-2-picryl-hydrazyl (DPPH) free radical [36]. Briefly, a freshly prepared DPPH solution in methanol as solvent (0.3 mM, 100 μl) was added to each sample (100 μl) with different concentrations in 96-well plate (n = 3). It worth noting that for the preparation of extract stock solution, 1 mg extract was dissolved into 1 ml methanol and serial dilutions were prepared from stock solution. The mixture was incubated in a dark place for half an hour. Next, the wavelength of DPPH was scanned by a UV–vis spectrophotometer (model UV2401; Shimadzu, Japan) at 517 nm. Ascorbic acid was considered as standard. Radical scavenging activity was calculated using following equation.

$$Capacity\ (\%) = \frac{\mathrm{Abs(control)} - Abs(sample)}{\mathrm{Abs(control)}} \times 100$$

$\mathrm{Abs}_{\mathrm{control}}$ is the absorbance of control, and $\mathrm{Abs}_{\mathrm{sample}}$ is the amount of absorbance of tested compounds and DPPH after 30 min. Data are reported as mean ± standard deviation (SD).

2.11. In-vivo wound healing study

The mice (mean weight 40 g) were chosen to investigate the scaffold biocompatibility. Animals have been put into standard cages and housed in humidity and temperature-controlled room (22 °C) with 12 h light-dark cycles and had free access to equal amounts of standard food and water, according to the Animal Ethics Committee of the National Institute of Genetic Engineering and Biotechnology, Iran. The ethical review number is IRNIGEB.EC.1402.11.29. The mice were anesthetized using ketamine (100 mgkg^{-1}) and xylazine (5 mgkg^{-1}). The dorsum of the mice was cut to put the scaffold on the wound directly. Wounds with the same size of 5 mm were created on the back of them using sterile standard punch and covered with to-be-tested scaffolds. The scaffolds were changed every three days. The process of wound healing was evaluated visually and photo-shooting was performed on days 0, 3, 7, and 14. The wounds were evaluated for the wound size reduction using Wilson's equation as follows [29].

$$wound\ closure\ (\%) = \frac{\mathrm{A0} - \mathrm{At}}{\mathrm{A0}} \times 100$$

Where A0 and At are the initial wound areas at postoperative day 0 and the wound area at the time of intervals, respectively.

2.12. Hematoxylin and eosin (H&E) staining

In order to perform histological analysis, at the day of 14, animals were euthanized through cervical dislocation and the skin, including the entire wound with adjacent normal skins, was excised and fixed in 4 % paraformaldehyde in PBS for one day. Once removed from the formaldehyde solution, tissue samples were washed with deionized water for 1 h. Then samples were dehydrated with 50 %, 70 %, 80 %, 90 %, 95 %, and 100 % ethanol solutions and xylene (to remove the alcohol) prior to embedding in paraffin wax. The tissue blocks were cut into 5 μm sections and then stained with H&E according to protocol expressed elsewhere [37]. The sections were then washed and visualized under a light microscope (Nikon, Eclipse TE2000-S, Japan). All experiments were performed with the ethical approval of the National Institute of Genetic Engineering and Biotechnology (Tehran, Iran) and in terms of their guidelines.

2.13. Statistical analysis

All experiments were performed in triplicate, and the mean ± SD was reported. Image J software was applied to calculate the diameter distribution of nanofibers. All data and graphs were analyzed using Graph Pad Prism 9, or Origin Pro 2020. The significance level of the difference between the groups was calculated as a p-value <0.05.

3. Result and discussion

3.1. Phytochemical analysis

Previous phytochemical studies on Verbascum plants have shown the presence of a wide range of secondary metabolites such as iridoid glucosides, sesquiterpenes [38], phenylethanoid glycosides [39], triterpenoid saponins, polysaccharides, flavonoids and terpenoids [40]. Verbascoside, as the most common phenylethanoid glycoside, isolated from the Verbascum genus, has strong antioxidant [41], antimicrobial [42,43], anti-inflammatory [44], cytotoxic activity against mouse P-388 cell line, And has also shown anesthetic and analgesic effects [45].

Pharmacological activities of iridoid glycosides, another class of secondary metabolites found in Verbascum species, have been reported for the treatment of degenerative rheumatoid arthritis, nephritis, arthritis, and heart disease [46] (see all abbrevated terms are defined in Table 1).

In the present study, we have obtained three fractions from crude extract of VT, namely *Aqueous, ethyl acetate and butanol* extracts. Since, an ideal wound dressing should have efficient antibacterial properties, we have tested the antibacterial properties of these extracts, in the first step, to find the best extract for NFM fabrication. Therefore, minimum inhibitory concentration (MIC) test using two bacteria, S. aureus and E. coli as a standard antibacterial test was performed for these extracts and the results are shown in Table 2.

The antibacterial activity of ethyl acetate, aqueous and *butanolic* and crude extracts was performed by the minimum inhibitory concentration (MIC) test using two bacteria, *S. aureus* and *E. coli*. According to the obtained results, the crude extract of the plant had antibacterial properties. The minimum inhibitory concentration was 250 μg/ml for *E. coli* and 125 μg/ml for *S. aureus*. Although, *ethyl acetate* and *aqueous* extract at higher concentrations had a slight effect on *S. aureus*, but they had no effect on *E. coli*. Meanwhile, *butanolic* extract showed significant antibacterial activity compared to the other three samples. The minimum inhibitory concentration (MIC) for this extract was 62.5 μg/ml (Table 2). Thus, based on the antibacterial assays on different fractions, *butanolic* extract was chosen as the best antibacterial fraction and was used for further tests.

The results of HPLC-UV chromatogram of butanol extract of VT is shown in Fig. 1. This chromatogram shows several peaks. HPLC analysis was performed and the samples identified at 254, 280 and 305 nm are shown in Table 3. Several peaks can be seen in the chromatogram sample and about 8 compounds were identified. Whereas, the 4-hydroxybenzoic acid (2.44 mgL^{-1}), caffeic acid (2.93 mgL^{-1}), *p*-coumaric acid (3.18 mgL^{-1}), cinnamic acid (1.07 mgL^{-1}) and ferulic acid (11.29 mgL^{-1}), were determined as the major phenolic acids and rutin (2.01 mgL^{-1}) as the major flavonoid. Among these compounds some unidentified peaks were observed with similar hydrophobicity and UV–vis pattern which are considered as the phenolic derived compounds. Total sample content was determined by HPLC and calculated using calibration curves based on the standards. These results can be related to the total content of phenolic compounds, which is one of the factors of antioxidant properties. Generally, phenolic compounds such as flavonoids and hydroxycinnamic acids, hydroxybenzoic acids such as gallic and ellagic acids are used as medicinal agents. As a result of the presence of these compounds, some plant extracts have anti-inflammatory and anti-cancer effects [47]. *p*-coumaric acid is a phenolic acid that has various biological activities including antioxidant, anti-inflammatory, analgesic and antibacterial properties. On the other hand, 4-Hydroxycinnamic acid is also a phenolic acid found in plants and vegetables. Its biosynthesis based on tyrosine leads to the formation of secondary metabolites and other phenolic acids such as caffeic acid and ferulic acid. The presence of these compounds in plants also leads to many properties including antibacterial antioxidant, anti-inflammatory, anti-cancer and pain-relieving properties [48]. Based on the results of HPLC test and confirming the presence of these compounds in V. thapsus extract, clinical and therapeutic characteristics can be generalized to it.

3.2. Scanning electron microscopy (SEM) of synthetized V.T-loaded NFM

SEM at an accelerating voltage of 26 kV under magnification of 5000 × was used to examine the morphology and diameter of prepared nanofibers. SEM images of the scaffolds in the final selected conditions and the diameter distribution diagrams of the nanofibers loaded with the different concentration of VT extract are given in Fig. 2. As it is observed, nanofibers have a cylindrical shape without any structural defects like beads or droplets when they are generated with spinning conditions of voltage 27 kV, distance 15 cm, and feeding rate 0.1 mL/h, Thereafter, these electrospinning conditions allowed the formation of a Taylor cone that is essential for the formation of nanofibers [49]. SEM images of the samples also indicated the successful formation of uniform, non-woven, randomly oriented round-shaped with smooth surface, and continuous NFs. The results of fiber diameter measurement using image J analysis software (Fig. 3) show the average fiber diameter of 186, 138, 126, and 103 nm for pure PVA, 2 %, 5 %, and 10 % VT loaded

Table 1
Abbreviations.

Abbreviations	
LB	**Luria-Bertani medium**
RPMI	**Roswell Park Memorial Institute (cell culture and tissue culture)**
FBS	**Fetal bovine serum**
NFM	**Nanofibrous membrane**
TFA	**Trifluoroacetic acid**
MeOH	**Methanol**
PBS	**Phosphate-buffered saline**

Table 2
The minimum inhibitory concentration (MIC) for 3 extracts of V. thapsus.

Concentration of extracts (μg/ml)																				
Test organisms	Crude extract of *V. thapsus*					Aqueous extract of *V. thapsus*					*Ethyl acetate* extract of *V. thapsus*					*Butanolic* extract of *V. thapsus*				
	500	250	125	62.5	31.2	500	250	125	62.5	31.2	500	250	125	62.5	31.2	500	250	125	62.5	31.2
Escherichia coli	–	+ (MIC)	+	+	+	+	+	+	+	+	+	+	+	+	+	–	–	–	-(MIC)	+
Staphylococcus aureus	–	–	+ (MIC)	+	+	–	+ (MIC)	+	+	+	–	+ (MIC)	+	+	+	–	–	–	-(MIC)	+

Key:=No bacterial growth; + = Bacterial growth.

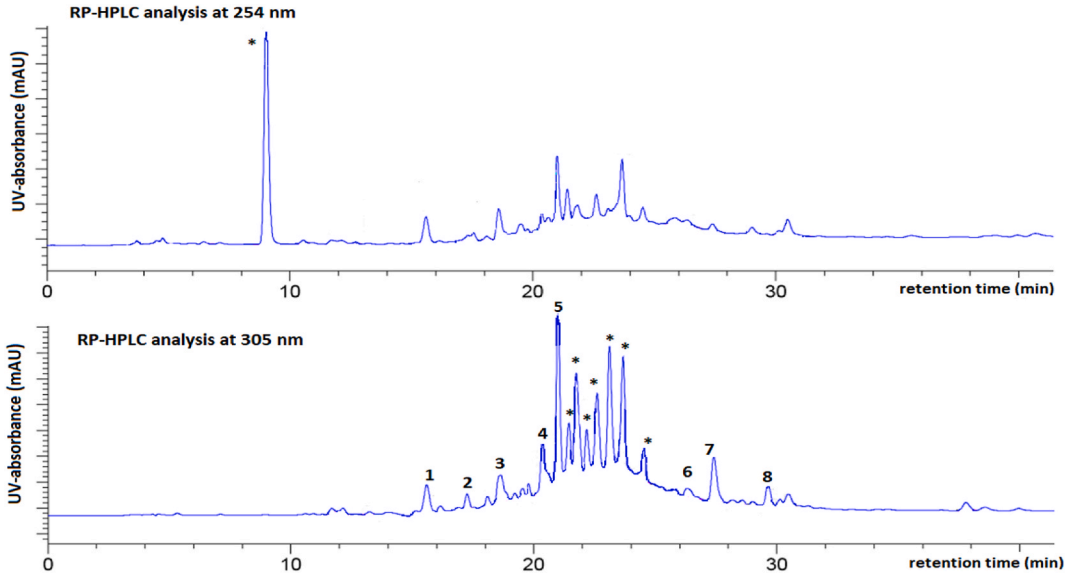

Fig. 1. Reversed phase HPLC analysis of fraction. at 254 and 305 nm; The column temperature: 25 °C. Flow rate: 0. 7 mL min−1. (1) gallic acid, (2) 4-hydroxybenzoic acid, (3) chlorogenic acid (4) caffeic acid, (5) *p*-cummaric acid, (6) Ferulic acid, (7) rosmarinic acid, (8) Rutin, (9) cinnamic acid, and (*) unknown compounds.

Table 3
Phenolic acids and flavonoids contents (mg/g of dry extract) in and *V. thapsus* extract.

Compounds	run time (min)	Area	mg/L of extract
4-hydroxybenzoic acid	15.6	196.5	2.44
chlorogenic acid	17.2	67.9	0.12
caffeic acid	18.6	223.8	2.93
p-coumaric acid	20.3	237.5	3.18
Ferulic acid	21.1	687.3	11.29
rosmarinic acid	26.4	39.1	trace
Rutin (280 nm)	27.3	172.8	2.01
cinnamic acid	29.7	120.6	1.07
unknown compounds	9.1	1683	-
	21.4	225.2	-
	21.7	548.9	-
	22.5	428.7	-
	23.1	664.7	-
	24.0	593.8	-
	24.5	151.2	-

NFM, respectively. This reduction may due to the anionic nature of extract caused by carboxyl and hydroxyl groups [50].

As it is known, higher charge density in electrospinning solution lead to higher electric conductivity and the ionic strength which in turn increases the elongation of the jet by the electrical field during electrospinning result in decreasing the nanofibers diameter. Fig. 3 illustrates the zeta potential of the extract solution in DI water. As it is observed, the zeta potential typically demonstrates negative values, therefore, confirm our hypothesis for fiber diameter reduction with increasing the extract content. Consequently, the charge of the desired polymer increases as the zeta potential decreases, resulting in a reduction in the diameter and thinning of the nanofiber [51, 52].

However, It was also observed that the loading of nanofibers with higher percent of extract could lead to the production of more ribbon like fibers which stuck together especially in 10 % case which may due to increase of polymer solution viscosity due to creation of higher hydrogen bonding between polymer molecules and extract component leading to sticking each other. Similar results were previously mentioned by Fahami et al. when using L. sativum/PVA NFs for encapsulation of vitamin A [51].

3.3. Fourier transform infrared spectroscopy (FT-IR) analysis

To investigate the chemical structural features and functional groups of VT extract, PVA, and VT-loaded PVA nanofibrous membranes (NFM), FTIR spectroscopy was utilized, and the resultant spectra are presented in Fig. 4. PVA is classified as a hydrophilic polymer owing to the presence of hydroxyl groups, which render nanofibers containing it unstable in aqueous solutions [53,54]. In the

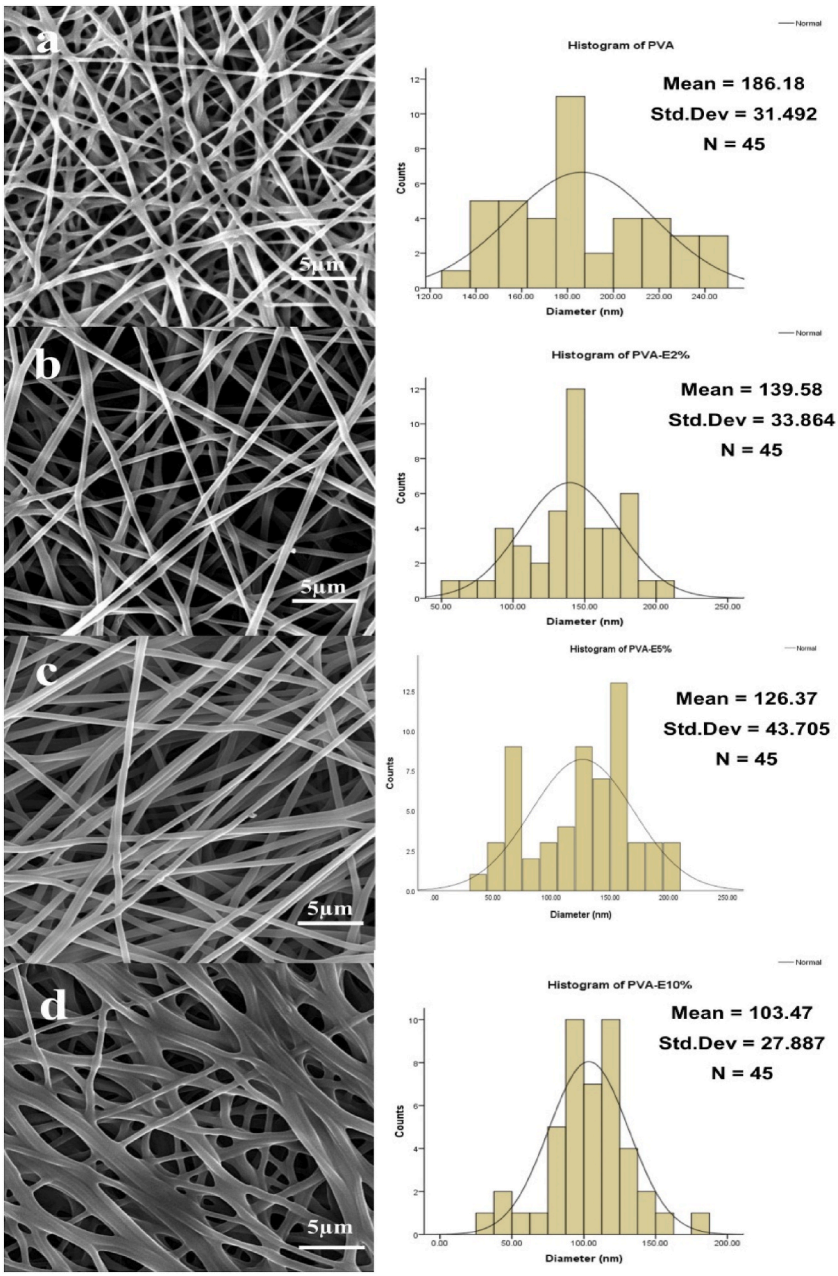

Fig. 2. SEM images and diameter distribution diagrams of nanofibers (a) PVA (b) PVA-E2% (c) PVA-E5% (d) PVA-E10 %, electrospun NFs and.

FTIR curve of PVA NFM, the observed peaks between the range of (3200 and 3550 cm-1) are connected to O–H from intermolecular hydrogen bonds, and the peak observed between 2840 and 3000 cm-1 is related to the C–H stretching of alkyl groups. Also, the observed peak of 1735 cm-1 is attributed to the carbonyl C–O group [55]. In the spectra of VT-loaded NFMs, there are some characteristic peaks related to VT extract, namely 655, 696,1510,2060, and 2256 cm-1 which indicate the loading of the extracts. But, as it is observed the most characteristic peaks of extract have been overlapped with PVA characteristic peaks and just slightly the intensity or position of peaks were altered possibly due to physical interaction with the polymeric matrix of the NFMs for example, the signals observed at 3368 cm-1 and 2942 for pure PVA, in the presence of plant extract has been shifted to 3319 cm-1and 2933 cm-1, which is due to the fact that these peaks represent hydroxyl groups and the functional groups of C–H, respectively that indicate the interaction of the mixtures with each other may through the formation of hydrogen bonding; Also, the observed peaks between the signal of 1520 and 1540 cm-1 in the VT-loaded NFM, which is also present in the FTIR curve of VT, show N–H bending related bond endorsing the encapsulation of extract in NFM structure efficiently [56–59]. All in all, the above mentioned results suggest successful entrapment of extract in NFM structure.

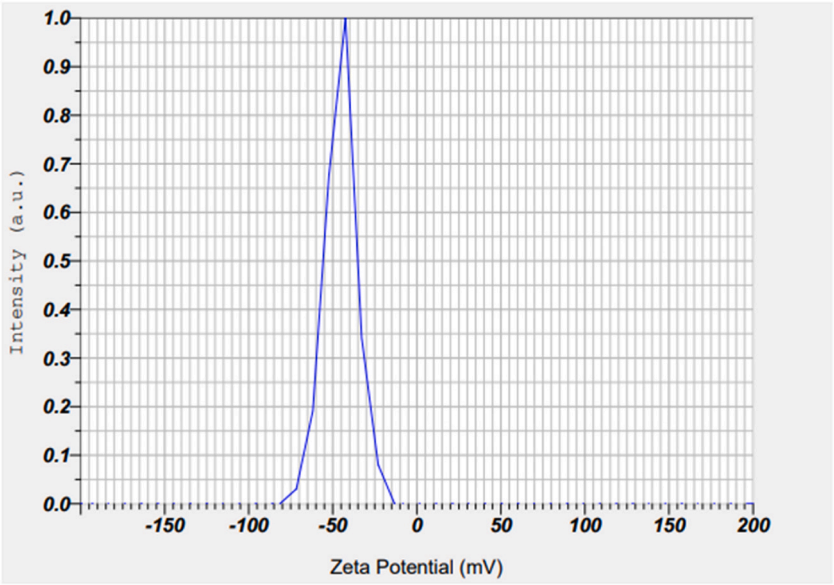

Fig. 3. Zeta potential values of dispersions with electrospun nanofibers.

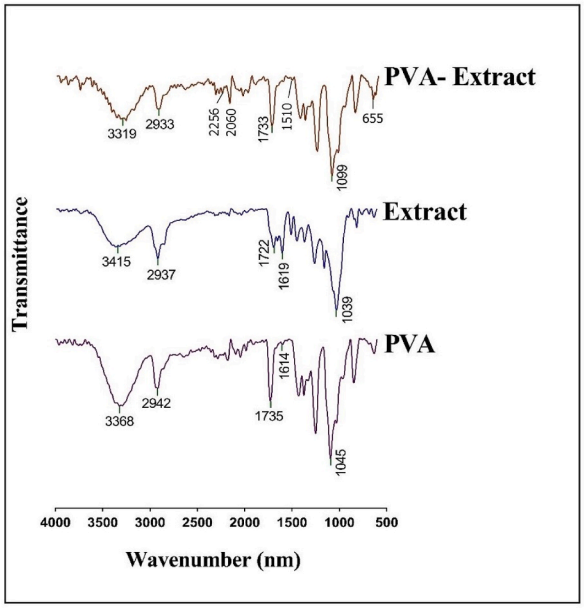

Fig. 4. FTIR spectra of PVA/Extract, crude VT and PVA electrospun NFs.

3.4. Contact angle measurements and surface wettability

The contact angle measurement of the prepared NFMs was assessed as an indicator of the hydrophilic-hydrophobic feature of them, which in turn can affect the absorption of exudates, maintaining the moisture in the wound site, cell adhesion, and proliferation [60–63]. The results are illustrated in Fig. 5. As it is observing, the drop contact angle decrease from around 39 ± 10° to 20 ± 8° for PVA and PVA-E10 %. This phenomenon suggests the hydrophilic nature of extract which with increase of it, the hydrophilicity of scaffold increases.

3.5. Water vapor transmission rate (WVTR)

An optimal wound dressing should maintain a moist environment to prevent dehydration and remove wound secretions.

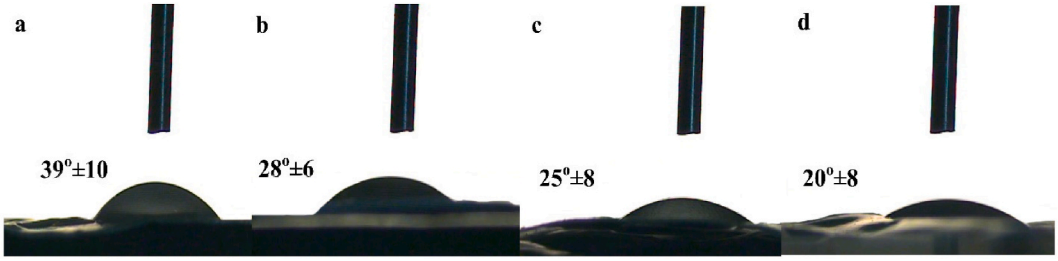

Fig. 5. Contact angle analysis, PVA (a), PVA-E2% (b), PVA-E5% (c), PVA-E10 % (d).

Accumulation of excessive tissue and secretions resulting from inflammation can lead to the breakdown of the extracellular matrix and impede wound healing [64]. Therefore, suitable wound dress should possess optimal properties similar to extracellular matrix of skin. It was reported that a desired scaffold for wound healing should support the WVTR of 2000–2500 g/m2/day [65]. In our case, the mentioned standard range was also obtained by fabricated scaffold. In consistence with other our results (Fig. 6a), surprisingly it is observed, the addition of 2 % of extract to the nanonofiber structure lead to increase of WVTR that can be related to decrease of

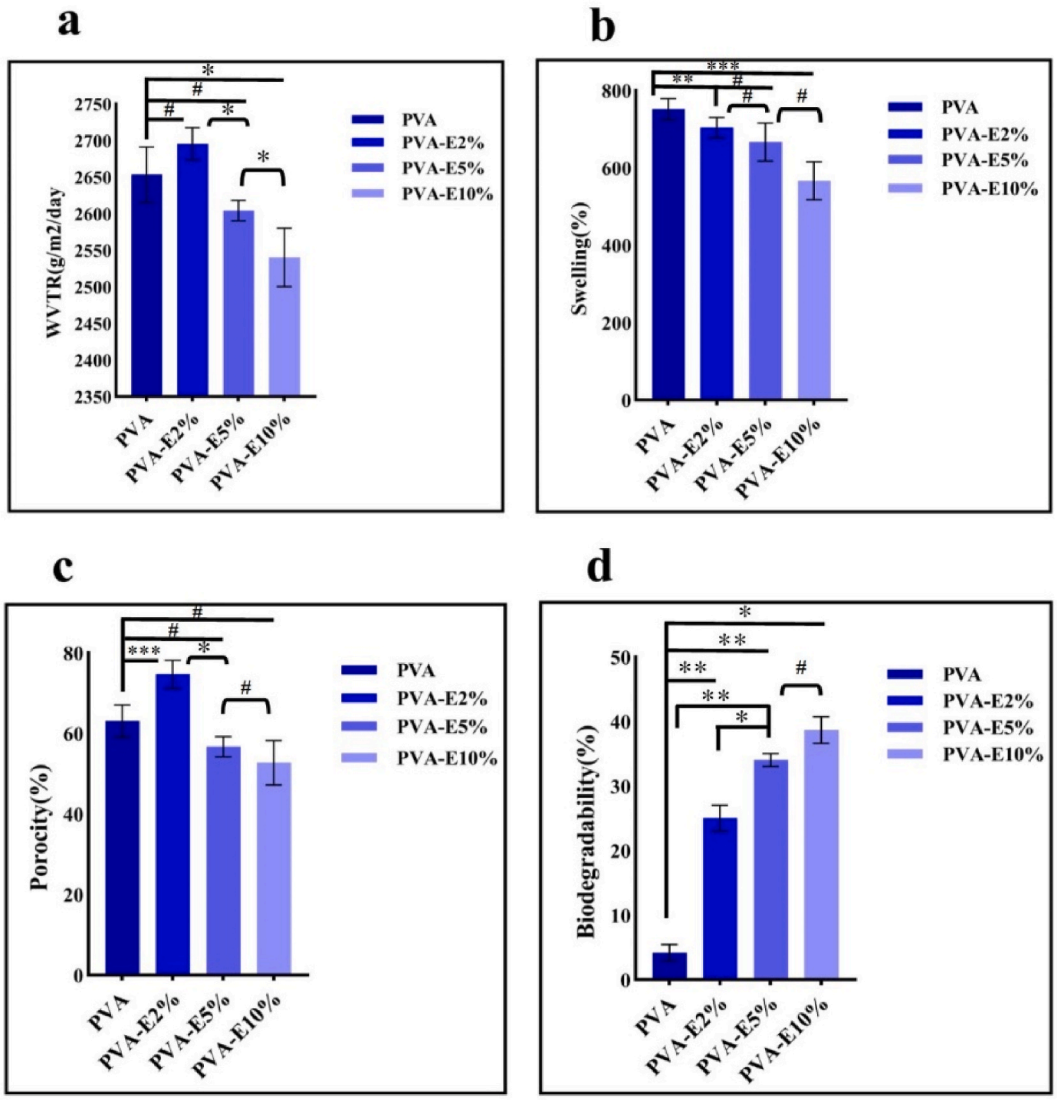

Fig. 6. WVTR (a), swelling ratio in PBS (pH = 7.4) (b), the porosity percentage (c), Degradation profiles (d). (n = 4, mean ± SD,* = P ≤ 0.05, ** = P ≤ 0.01, *** = P ≤ 0.001 and Label # shows insignificant difference between data).

nanofiber diameter thereby facilitating enhanced air permeability, as also approve in SEM images. However, with increase of extract content it was observed that WVTR tends to decline. The augmented adhesion between nanofibers owing to the added extract decreases the inter-chain distance, consequently leading to a diminution in air permeability [66]. On the other hand, an increase in the extract content leads to the formation of additional cross-links, resulting in a decrease in the swelling of the scaffold. Reduced swelling in the membrane impedes the greater air and steam passage [28,29]. By the way, all the fabricated NFMs can support the mentioned optimal WVTR for wound dressing.

3.6. Swelling

Discrepancies in swelling behavior were noted between the membranes loaded with the extract loaded and the control samples, as illustrated in Fig. 6b. Through the addition of extracts to nanofibers, the degree of swelling decreases. This is attributed to the bonding and cross-linking of the extract molecules with polymer chains, subsequently reducing the swelling of nanofibers. Swelling in nanofibers occurs due to the expansion of polymer chains and the trapping of water within them, thereby leading to swelling. Nonetheless, the presence of the extract in conjunction with nanofiber polymers averts this process and mitigates swelling [65]. The control PVA membrane displayed a swelling percentage of 700 %, whereas the PVA-E2%, PVA-E5%, and PVA-E10 % samples demonstrated reduced swelling rates.

3.7. Porosity

The extracellular matrix, enveloping cells in human tissues such as the skin, constitutes a nanostructured environment comprised of protein strands. These strands construct a three-dimensional matrix that supports cell binding, proliferation, and differentiation. In crafting an ideal scaffold, it is imperative to emulate the attributes of the extracellular matrix, encompassing its nanostructure size, porosity, and three-dimensionality [67]. The porosity of scaffolds plays a critical role in tissue engineering initiatives by providing void spaces for cellular accommodation and migration. Furthermore, it enables the exchange of vital elements such as nutrients, fluids, and gases [68].

The results obtained illustrate the porosity of the PVA, PVA-E2%, PVA-E5%, and PVA-E10 % scaffolds as depicted in Fig. 6c. As it is mentioned above, SEM images suggests that as the extract concentration increases, there is a rise in fiber adhesion, potentially leading to a higher density of nanofibers (due to the apparent fusion of multiple nanofibers into a single, larger fiber). The diameter of nanofibers in the sample containing 2 % extract, when compared to pure PVA, has exhibited a decrease, attributed to the concomitant increase in porosity. Subsequently, with escalating concentrations of the extract in the PVA-E5% and PVA-E10 % samples, a decrease in porosity is observed. This phenomenon can be ascribed to the heightened cross-linking interactions between the extract and polymer chains, coupled with enhanced adhesion among nanofibers. Thus, in consistent with existing literature, an augmentation in nanofiber size is linked to a reduction in porosity [36].

3.8. Degradation

The degradation rate of wound dressings should be carefully regulated to align with the temporal dynamics of new tissue formation, allowing for sufficient duration to facilitate skin regeneration. Deviations towards excessive or insufficient degradation can lead to adverse outcomes such as compromised mechanical adaptability at the cellular interface and compromised tissue integrity [69]. The degradability of the samples was evaluated, and the results are depicted in Fig. 6d. It is apparent that the weight loss ratio of all samples exhibited a progressive increase over time, with the nanofibers showing a notable decrease in their initial weight after 30 days of immersion in the buffer solution. In the case of the PVA sample, its polymer chains remained unchanged due to their cross-linking and

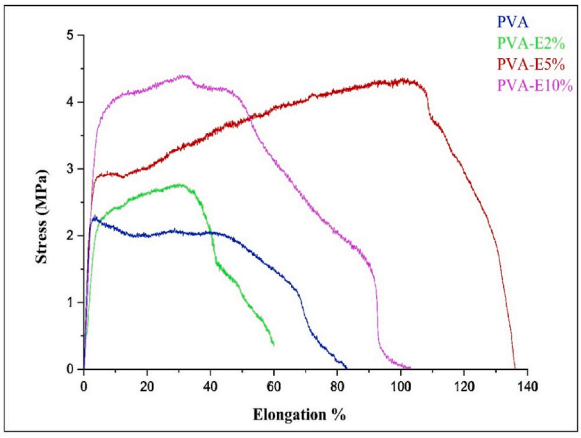

Fig. 7. Mechanical properties of PVA and PVA/VT nanofiber membranes.

limited biodegradable nature. However, the incorporation of extract into the nanofibers resulted in an acceleration of the degradation process. In biodegradation process, factors such as porosity and morphology play pivotal roles in influencing the degradation mechanism. Within the samples comprising PVA-E2%, PVA-E5%, and PVA-E10 % extracts, the release of the medication from the nanofibers resulted in its dispersion into the adjacent solution and surroundings, causing a reduction in the mass of the nanofibers and a simultaneous increase in degradability. Notably, the sample containing a 10 % extract exhibited the highest level of biodegradability a phenomenon likely attributed to the extraction of the extract from the nanofiber matrix, thereby instigating the formation of voids within the membrane, rendering it more susceptible to degradation [60].

3.9. Mechanical properties

An ideal wound dressing should possess ideal mechanical features such as flexibility, hardness, and mechanical properties compatible with human skin. To evaluate this, the mechanical properties of the investigated scaffolds were assessed [32]. The outcomes of this evaluation for PVA, PVA-E2%, PVA-E5%, and PVA-E10 % samples are depicted in Fig. 7. The control sample, PVA, exhibited an elongation rate of approximately 80 %. The addition of a hydrophilic alcohol-based VT extract, which enhances the hydrophilicity of nanofibers, resulted in increased elongation and strength in the other samples [70].

As it is also discussed in SEM results analysis, it was revealed that higher extract concentrations led to increased viscosity and increased fiber adhesion. Consequently, the tension between nanofibers increase due to increase if active cites for bonding, promoting the cross-linking of polymer chains, enhancing strength by restricting movement and reducing elongation [32]. In PVA-E5%, an increase in the strength and elongation of nanofibers was observed due to higher extract content and reduction in fiber diameter. The PVA-E10 % samples exhibited sticky characteristics and higher viscosity, resulting in reduced fiber movement, smaller fibers, and increased adhesion, consequently decreasing elongation [71]. Therefore, the incorporation of VT extract into nanofibers has the potential to enhance the mechanical properties of membranes, making them suitable for wound dressing applications.

3.10. Antibacterial study

Bacterial infection in skin wounds is one of the most critical challenges in treating infections caused by it since the excessive use of antibiotics increases the resistance of bacteria to antibiotics; paying attention to the antibacterial wound dressings based on nanofibers made with plant extract can be of high interest. As it is mentioned before, bacterial infection is the main reason of wound infections; therefore, the base for our extract choice for wound healing application was the most efficient one in antibacterial activity. Based on our initial evaluation, *butatolic* extract VT has the higher antibacterial properties thus it was chosen for NFM fabrication for wound dressing applications. Therefore, the antibacterial activity of the dressing's mats was evaluated prior to being used for the healing of injured wounds. The antibacterial activities of NFM loaded with different concentration of *butanolic* extract (0, 2, 5, 10 %) were determined against Gram-negative, Escherichia coli (denoted as *E. coli*); and Gram-positive, *Staphylococcus aureus* (denoted as

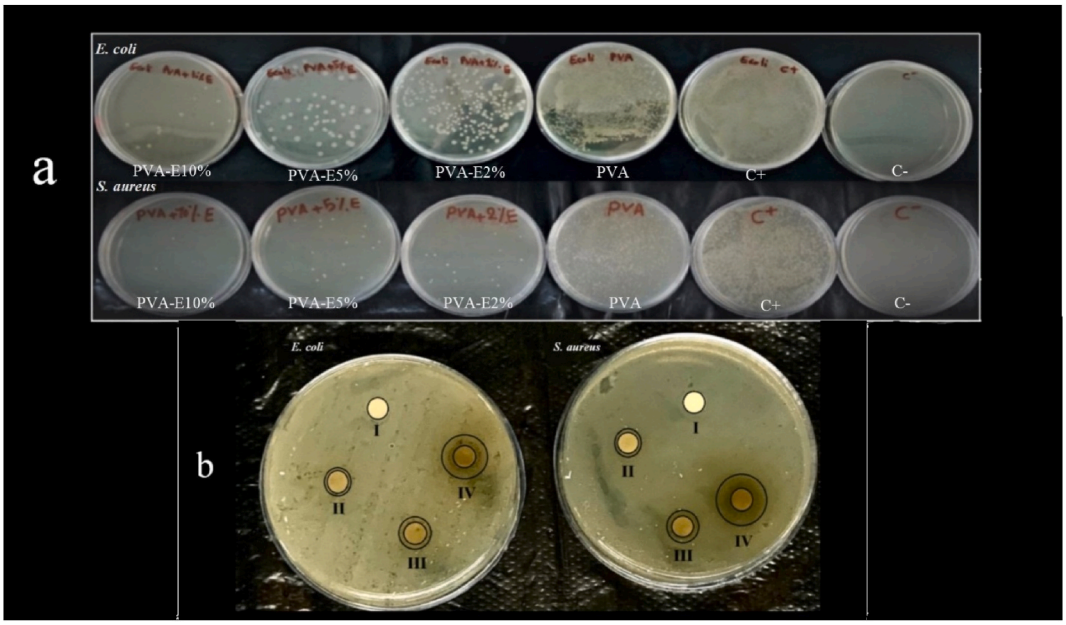

Fig. 8. a) Antibacterial activity (normal saline test) of scaffolds with different percentage of VT extract against Gram-negative, Escherichia coli (denoted as *E. coli*); and Gram-positive, Staphylococcus aureus (denoted as *S. aureus*). b) Inhibition zones for PVA-VT samples against bacterial pathogens *E. coli* and *S.aureus*, after 24 h incubation. I) PVA, II) PVA-E2%, III) PVA-E5%, IV) PVA E10 %, Initial diameter for all the disk samples is 10 mm.

S. aureus). In this regard, the fate of bacterial activity, when they are placed in the vicinity of different NFM in saline solution for 4 h is shown in Fig. 8a. When electrospun nanofibers with the extract of VT are placed in the vicinity of bacteria in saline solution media, they show remarkable antibacterial properties which are improving with the increase of extract percent in NFM compared to the bare scaffold. The same result for antibacterial properties also reported elsewhere for VT crude extract obtained by aqueous solvent [72].

To confirm the antibacterial properties of fabricated NFMs, inhibition zone assay was also performed on samples. The results of this test are presented in Fig. 8b. These results are consistent with the minimum inhibitory concentration (MIC) and the normal saline test. As shown, the control sample (PVA) did not exhibit any inhibition zone against *E. coli* and *S. aureus* bacteria, whereas the VT-loaded samples demonstrated a clear inhibition zone. The diameter of the inhibitory zones on *E. coli* increase with increase of extract percent in membrane from PVA-E2% to PVA-E10 % samples. As it is mentioned previously, VT species contains a wide range of compounds, such as glycosides, alkaloids, phenols, flavonoids and saponins that all of them have antibacterial properties. For example, it has been reported that phenols inhibit the enzyme of oxidized compounds, and probably through reaction with sulfhydryl groups or through non-specific interactions with proteins, they affect bacteria mechanism of action and create antibacterial activities [73]. The antibacterial tests showed that nanofibers loaded with VT were effective against both *S. aureus* and *E. coli* and could inhibit their activity with high degrees. Interestingly, the combination of nanofibers and VT extract shows a significant reduction in bacterial colonies in different concentrations. This result shows that the fabricated nanofibers can act as antimicrobial scaffolds for wound healing.

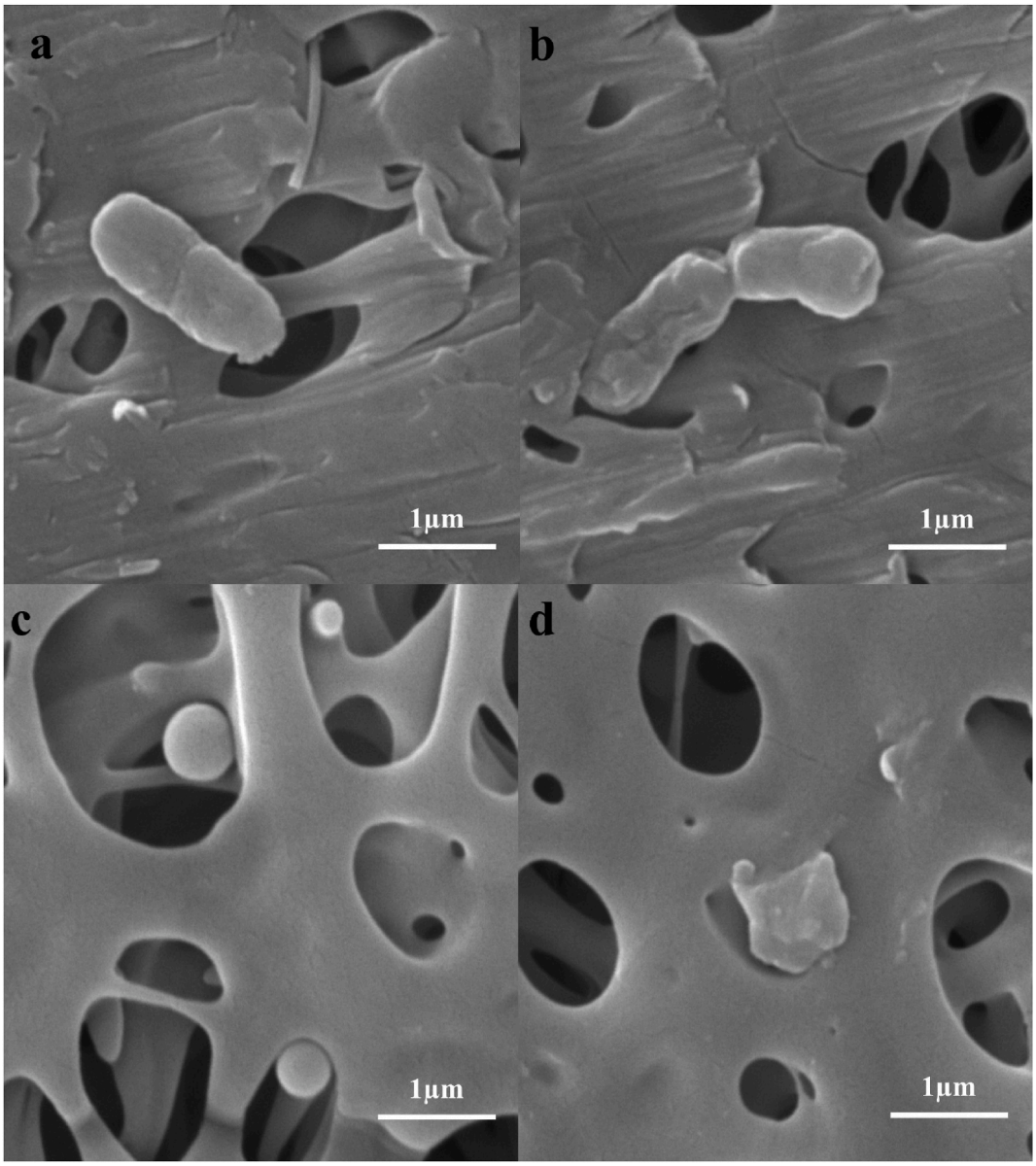

Fig. 9. SEM images of bacteria, untreated E. coli (a), treated E. coli with PVA-E5% (b), untreted S. aureus (c), treated S. aureus with PVA-E5% (d).

Furthermore, as it will be discuss in the following sections, cell viability confirms that the antimicrobial activity of the fabricated scaffolds is due to their actual antibacterial activity and not to their cytotoxicity [30].

In addition, the effects of nanofibers synthesized with a certain percentage of VT extract on the morphological changes of *E. coli* and *S. aureus* bacteria were also investigated by SEM. Fig. 9 shows the results of this study. As it is clear from this figure, untreated *E.coli* has a rod-like structure and has a smooth and untouched surface. However, the morphology of these cells was significantly changed and damaged when exposed to NFM loaded with VT extract (Fig. 9b). After passing the incubation time in the vicinity of NFM, the covering and the cell wall became uneven and took on an unusual shape resulting in a serious injury has created holes and indentations in the cell membrane and its integrity has been completely lost. Similarly, Fig. 9c shows the untreated *S. aureus* cells that have kept their spherical, smooth and regular shape naturally. However, Fig. 9d of *S. aureus* cells treated with VT loaded NFM shows significant changes and damages to *S. aureus*. Irregularity, low depth and indentation in the cell membrane and rupture of the cell wall are completely visible. SEM analysis showed that *S. aureus* and *E. coli* cells were damaged and destroyed when exposed to nanofibers containing extracts. The obtained results can be attributed to the antibacterial property of VT loaded in NFM.

3.11. MTT assay

Alkaloids are heterocyclic organic compounds found in more than 6000 plant species as secondary metabolites [74]. Alkaloids are often toxic, and this toxicity is structure-dependent because a double bond in the nesine base, making it unsaturated, that have more significant toxicity compared to saturated nesine bases. Alkaloids are primarily stored as protoxins in the plant in the form of benign N-oxides, while in the digestive tract of animals, they are reduced to amines, which have toxic effects [75]. It has been reported that spermine alkaloid is present in the composition of *V. thapsus* plant [76], and these alkaloids are cytotoxic for cells. But it was reported [77], that the use of a series of solvent systems, such as ethyl acetate-butanol-water removes the alkaloids in the extract [78].

In the present research, the solvent purification method was used to reduce the alkaloids contain of obtained extract and neutralize their toxic effects. In order to assay the cytotoxicity of obtained extract and also fabricated NFM, MTT assay was performed on L929 cells. Based on Fig. 10a and b, the result indicated that L929 cell shows better viability and proliferation in the presence of lower concentration of extract may due to incomplete elimination of alkaloid compound in the extract. On the other hand, in the all of VT-loaded scaffolds, L929 shows significant proliferation compared to the pure PVA NFM and had a time-dependent growth pattern and increased cell growth. However, it seems that on PVA-E5% enjoy the less cytotoxicity due to the presence of optimum concentration of VT loaded in its structure. Therefore, the use of electrospun NFs with optimal concentration of extract can have more medicinal properties with less toxicity.

3.12. Hemolysis assay

To check the biocompatibility of electrospun samples, the blood hemolysis assay was carried out against human blood. Fig. 10c shows the results of this test for PVA, PVA-VT2%, PVA-VT5% and PVA-VT10 % samples. As can be observed in the figure, the hemolysis percentage of the samples is below one percent. According to a study conducted in 2019 by Prakash et al., it was reported that the amount of hemolysis less than 5 % can be a suitable range for biomaterials. Based on this, it can be mentioned that all the electrospun nanofibers in this study are biocompatible [71].

3.13. Cell proliferation study by SEM and DAPI examinations

A promising wound dressing needs to be able to support cells to proliferate on a scaffold. One of the basic approach to this assess

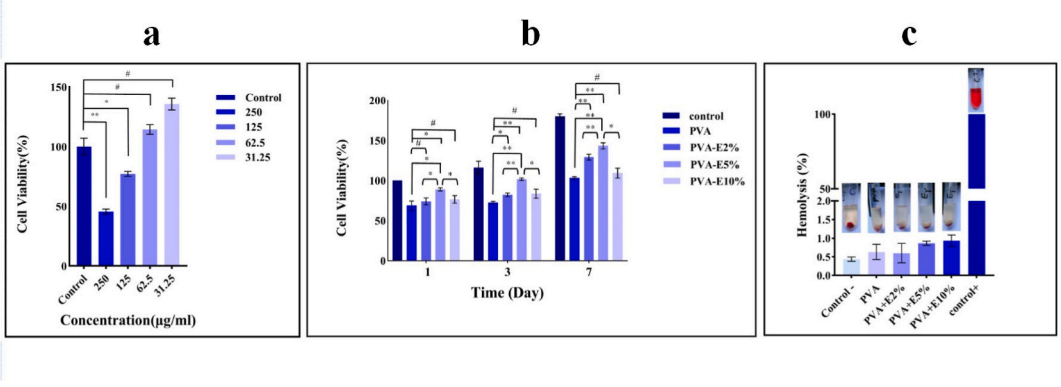

Fig. 10. Cell viability (MTT) of L929 fibroblast cells on the VT extract with different serial dilutions (a) Cell viability (MTT) of L929 fibroblast cells on the Control (Tissue Culture Plate), PVA, PVAE2% (E1), PVA-E5% (E2) and PVA-E10 % (E3) electrospun NFs after 1, 3, and 7 days of culture. (b) Test of PVA, PVA-E2%, PVA-E5%, PVA-E10 % and control hemolysis of electrospun NFs (c). (n = 4, mean ± SD,* = P ≤ 0.05, ** = P ≤ 0.01 and Label # shows insignificant difference between data).

this feature of scaffold is the SEM study at different time point after cell seeding on scaffold. For this purpose, SEM imaging was performed on fabricated scaffold on day 1 and 3 after cell seeding. Fig. 11 shows the state of cells on the different types of membranes at first and third days. As this figure confirmed, the number of cells attached to the nanofiber membrane containing the extract has a relative increase compared to the pure PVA NFM completely in line with MTT results. Also, it is obvious that nanofibers containing 5 % of the extract (VT) provides a better and wider spread of cells. As a result, it can be mentioned that this amount of extract in the nanofiber membrane was more compatible with the cells. In addition, the results obtained from DAPI staining also confirm the results of MTT and SEM analysis. As shown in Fig. 11 the cells proliferation is prominent on scaffolds loaded with VT extract.

3.14. *In-vitro scratch wound assay*

L929 cell ability to migrate and cover the gap created on the surface of cell culture plate in the presence of 3 days VT-loaded NFM juices, was study through classic in-vitro scratch assay. The captured images of wound healing kinetics and the wound closure procedure of all five types of samples at incubation time intervals of 0 h, 24 h, and 48 h is shown in Fig. 12. As it is evident, VT extract have a key role in wound healing and closure of gap. In addition, it is obvious that all VT contained samples accelerated the speed of gap closure after 24 and 48 h in comparison to the neat PVA sample or control. This can be ascribed to the presence of VT within the PVA nanofiber. Interestingly, again PVA-VT 5 % sample is benefited a higher recovery rate compared to the other samples. Similar results were also reported in other studies. For example, hydroalcoholic *V.thapsus* extract has shown a healing effect on the skin wound and the regeneration of the epidermis layer at the wound site [6]. Based on these results VT-loaded PVA scaffolds could be a good choice for

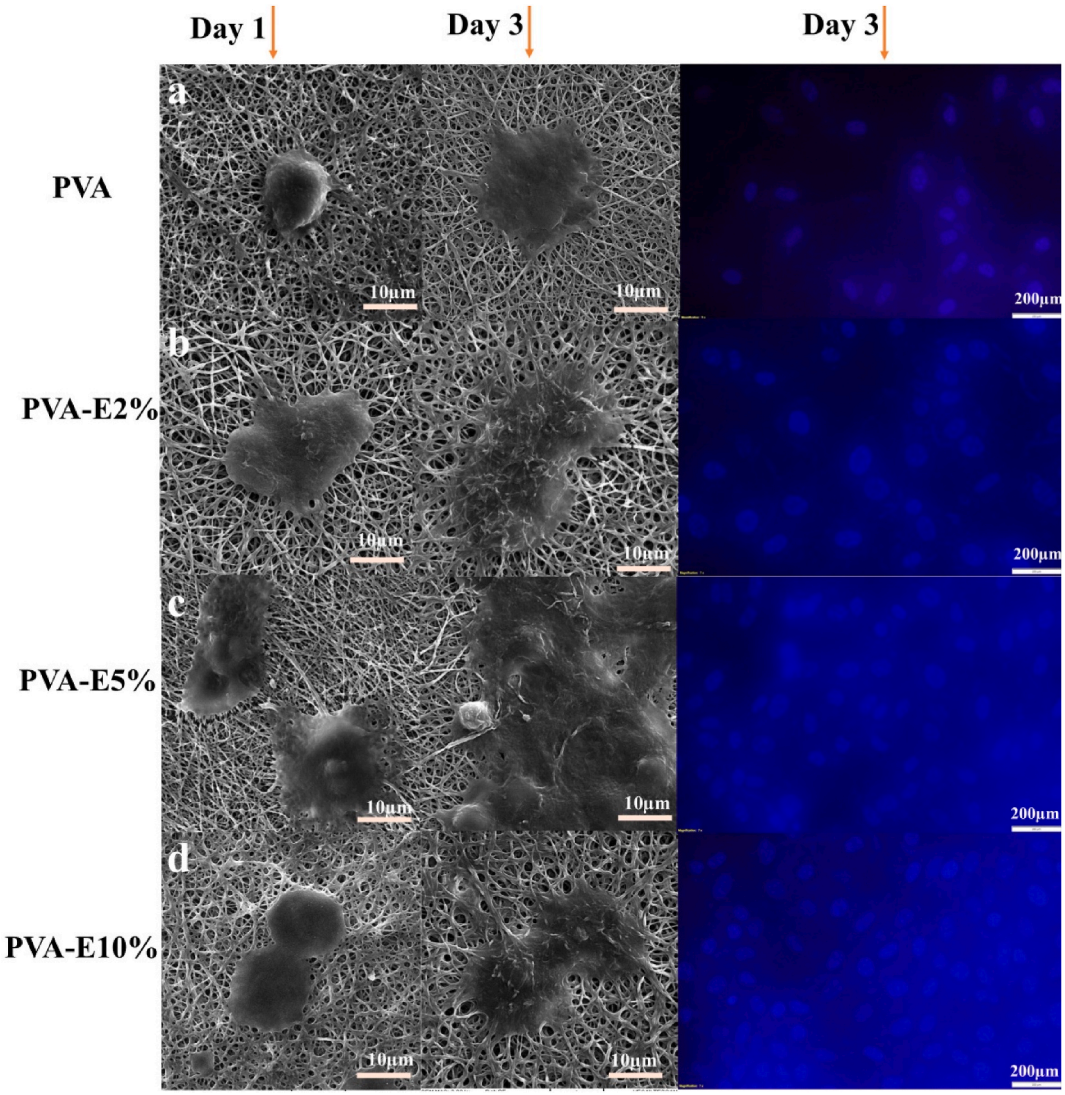

Fig. 11. SEM image of dispersion and spreading of L929 cells attached to the NFs membrane on the first and third days (a). PVA (b), PVA-E2% (c) PVA-E5% (d), PVA-E10 %, and DAPI staining test PVA, PVA-E2%, PVA-E5% and PVA-E10 % on the third day.

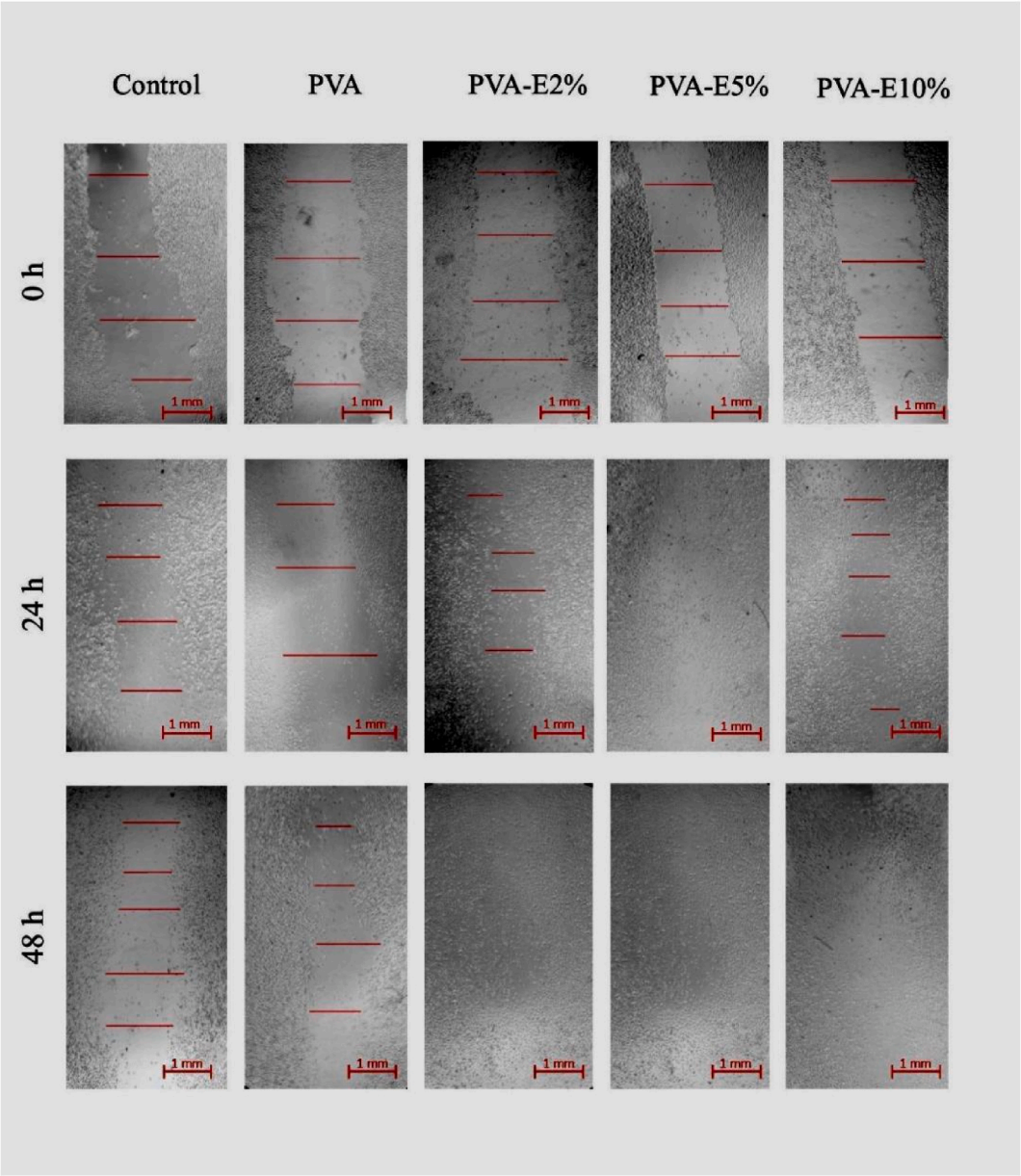

Fig. 12. Wound scratch assay of control, PVA, PVA-E2%, PVA-E5% and PVA-E10 % electrospun NFs after 0 h, 24 h, and 48 h.

wound dressing by influencing the wound healing process. Also, these nanofibers can reduce treatment costs in addition to their effect on wound treatment [79]. Recent scientific research on *V. thapsus* has shown through various experimental studies that it possesses a range of biological and pharmacological qualities. These include antiviral, antioxidant, analgesic, sedative, anti-inflammatory, hypnotic, antibacterial, antifungal, and even anticancer properties [6,80–82].

3.15. Determination of antioxidant activity (DPPH)

Free radicals usually have unpaired electrons in their outer orbit. They are highly reactive and take electrons from other compounds and convert themselves into stable molecules. However, due to the generation of free radicals, this reaction can cause cytotoxic effects. Antioxidants are molecules with stability that can neutralize free radicals by donating electrons. Therefore, the risks of oxidative damage are reduced by them [83]. For this purpose, to check the antioxidant activity of electrospun samples of PVA, which contain different percentages of VT extract, DPPH radical inhibition test was performed. Fig. 13 shows the percentage of antioxidant activity of these samples. Based on this figure, it can be observed that the antioxidant activity of VT extract is high in different concentrations; and the electrospun samples containing the extract have an acceptable antioxidant activity. The PVA sample without VT extract has a lower

antioxidant activity than the samples containing the extract. It is obvious that increasing the amount of extract in nanofibers increases their antioxidant activity up to 70 or 80 %. This result shows that these nanofibers can act as a barrier to producing reactive oxygen species in wound site and may help reduce the side effects of wounds and their faster healing.

3.16. In vitro drug release study

Fig. 14 shows the extract cumulative drug release from PVA-E2%, PVA-E5% and PVA-E10 % in PBS with pH 7.4. The dose of VT released in the first hours of release is due to the placement of the extract on the surfaces of the outer layer of NFs, which is considered low compared to other forms of polymeric drug carriers. The release rate of the extract has continuous and stable diffusion, which is attributed to the electrostatic interaction between positive and negative charges between VT and PVA molecules in NFs. Slow release of extract from NFs can significantly improve and accelerate wound healing rate compared to fast release [84]. The gradual release and diffusion of the plant extract stimulate the migration of skin cells, and following its further diffusion, microbial cloning is prevented after 24 h. Slow release of bioactive components due to changing the wound dressing once or twice a week, depending on the depth of the injury, can be beneficial [85]. In this condition, there is always a sufficient amount of extract in the wound area, which can be effective in the wound healing process [86].

3.17. In vivo wound healing assessment

Tissue repair is a process in which growth factors induce cell proliferation. During this process, there are changes in soluble mediators, blood cells, extracellular matrix production, and proliferation of parenchymal cells. The cellular and biochemical stages of wound healing have four main stages: homeostasis, inflammatory reaction, cell proliferation, and remodeling stage, in which the extracellular matrix is formed. These steps can overlap over time as well as with cells, growth factors, and cytokines that participate in

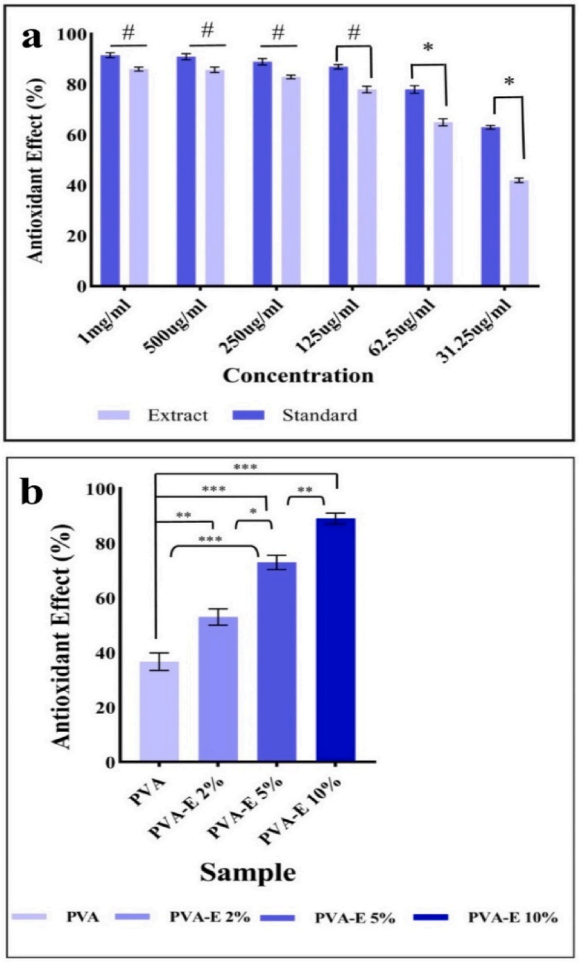

Fig. 13. Antioxidant activity of VT extract with different dilutions and, PVA, PVA-E2%, PVA-E5%, PVA-E10 % electrospun NFs. (n = 4, mean ± SD, * = P ≤ 0.05, ** = P ≤ 0.01, *** = P ≤ 0.001 and Label # shows insignificant difference between data).

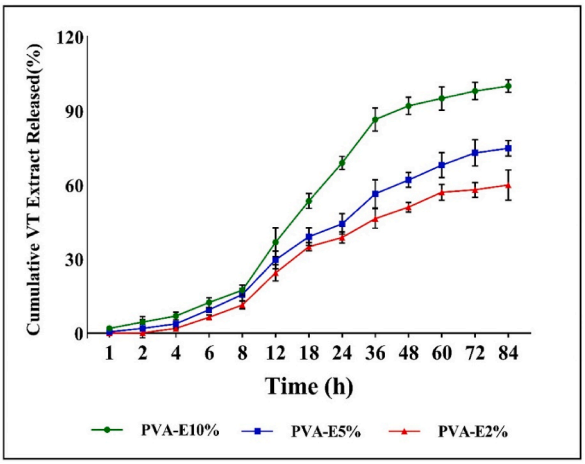

Fig. 14. Cumulative extract released profiles of PVA-E2%, PVA-E5% and PVA-E10 %.

the tissue repair process [87].

In this study, full-thickness circular wounds (5 mm) were created on the back of mice. Representative photographs of wound healing at different time points are shown in Fig. 15a. Most of the wound tissues of the control group and the other three groups shrank in 14 days, however, for the control and PVA groups, a small amount of infection was observed on the seventh day. The effectiveness of the wound is measured by measuring its diameter over a certain period of time. After the 7th day, wound closure in the control group was 31.7 %. This is while the percentage of wound closure in the samples treated with nanofibers containing PVA-E2%, PVA-E5% and PVA-E10 % extracts was 27 %, 50.2 % and 32.2 %, respectively, and also in the PVA control sample, this number was 11.2 %. The percentage of wound contraction and healing increased after 14 days in all groups. After this period of time, the control sample showed 33.8 % healing, and the groups containing PVA-E2%, PVA-E5%, and PVA-E10 % nanofibers showed 38 %, 68 %, and 36.4 % wound healing, respectively (Fig. 15b). It is also known that the healing rate of wounds treated with PVA as a control was lower than other scaffolds containing extracts. The wound treated with PVA-E5% had the fastest healing that this is completely in line with other result of in-vitro assessment. Therefore, it seems that 5 % loading of VT in nanofibrous structure is optimum concentration for wound dressing applications. Various effective compounds in Verbascum plant species, such as flavonoids, polysaccharides, tannins, saponins, verbacosides, steroids, and carbohydrates, have anti-inflammatory and antimicrobial properties and are essential factors in wound regeneration [45].

According to the results of extracting the chemical compounds of Verbascum, the flavonoid is an abundant compound in this plant. Flavonoid-related wound healing mechanisms include increased vascular endothelial growth factor (VEGF), hydroxyproline, and anti-inflammatory effects. Extraction of phenol in Verbascum extract shows its effect on the wound healing process [11]. Plant extracts containing many phenolic compounds have significant antioxidant, antibacterial and anti-inflammatory activity and are considered an effective option in the rapid repair of damaged skin tissues. In addition, it causes collagen synthesis by fibroblasts and helps increase the wound's strength [88]. Furthermore, optimal wound dressing should provide a moist environment to prevent dehydration and eliminate wound secretions [89].

3.18. H&E staining

As it is also mentioned above, the wound healing process is remarkably complex and depends on various factors; it is generally divided into four overlapping but distinct phases. These stages include homeostasis, inflammation, proliferation, repair, and finally, wound regeneration [90].

In physiological wound healing, keratinocytes begin to migrate centrally from the edge of the wound. It worth noting that, the stages of proliferation and migration of epidermal cells is the most critical repair processes in wound healing. Epidermal cells at the wound's edges destroy their connections to other epidermal cells and the basement membrane by changing their structure. The migration of epidermal cells is usually single, which is affected by the polar contraction cycles of the cytoskeleton [91].

In this study, H&E staining was performed to investigate the histology and biocompatibility effect of fabricated NFM on wound healing process. Fig. 16 shows the histological sections of mouse skin and the healing process in four groups after 14 days of wound creation and treatment. As shown in the figure, the integrity of the scaffold is lost and bio-absorption is observed. In the control group and PVA the formation of epithelial lining (REP) on the surface of the wound is weak and there is no epithelial lining in a large part of the surface of the wound. According to what is shown in the figure, the formation of granular tissue (Gn) is quite clear. In the PVA-E2% group a thin epithelial coating (about 1–2 cell layers) was created on the surface of the wound and the granular tissue was also evident. PVA-E5% group and PVA-E10 % group show the highest healing rate. In the PVA-E5% group, an epithelial coating was created on the wound surface and the dermis and its appendages including hair follicles, structures and secretory glands (dermal adnexa/appendages) were formed. In the PVA-E5% group, the epithelial lining is also formed. It seems that dermal appendages including hair follicles,

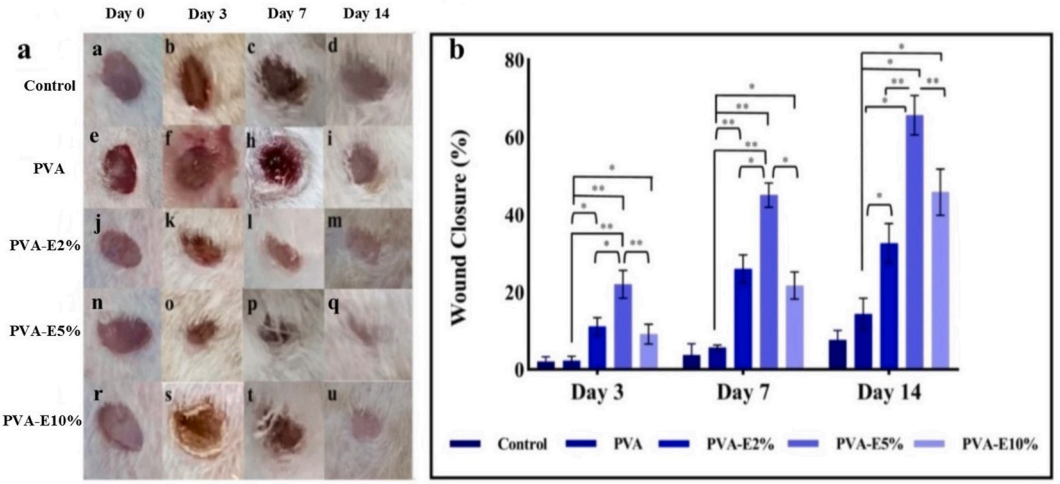

Fig. 15. Visual observation of control, PVA, PVA-E2%, PVA-E5% and PVA-E10 % wound healing in a mouse excisional wound model (a), Quantitate evaluation of wound healing closure over time 0, 3, 7 and 14 days (b). (n = 4, mean ± SD,* = P ≤ 0.05, ** = P ≤ 0.01 and Label # shows insignificant difference between data).

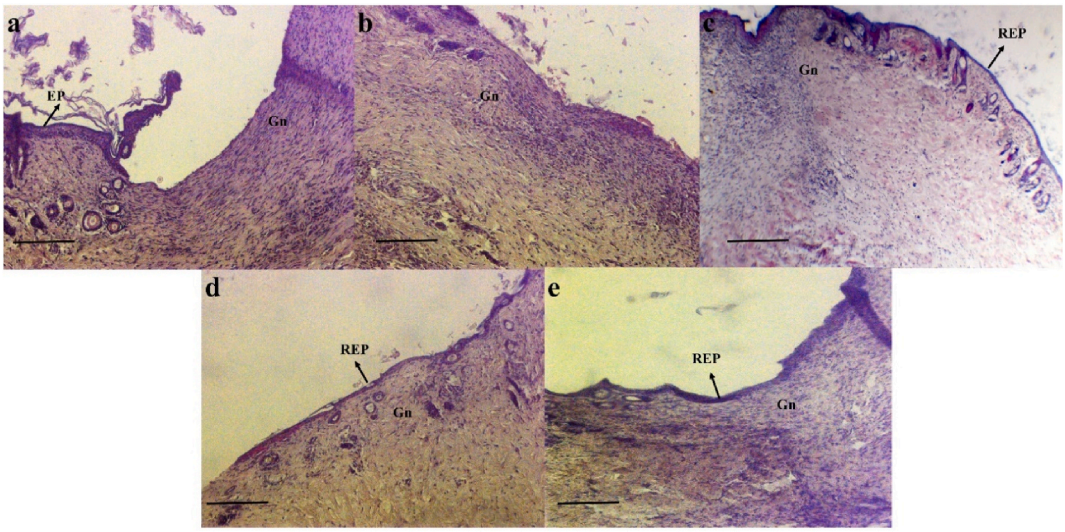

Fig. 16. Photomicrographs of skin tissues with H&E staining on days 7 and 14 of wound healing for control (a), PVA (b), PVA-E2% (c), PVA-E5% (d), PVA-E10 % (e).

structures and secretory glands (dermal adnexa/appandages) are formed only in the marginal repaired areas. According to the results of mouse wound healing in the in vivo test that was done for the actual effect of wound healing and also considering the results of antibacterial properties and biocompatibility, this evidence can confirm that the addition of VT extract to nanofibers increases the wound healing properties.

4. Conclusion

This study presented a novel bioassay guided fractionation protocol which was efficient and effective in screening *V. thpsus* extract as an antibacterial polyphenolic fraction and then successfully VT/PVA nanofibers with different ratio was developed as wound dress. Comprehensive physicochemical, in-vitro and in-vivo characterization of these scaffolds revealed they are efficiently biocompatible. The evaluation of these nanofibers on mouse wounds shows that wound healing process in the experimental groups is more effective than control group one. Meanwhile, the promising results of these electrospun nanofibers in increasing cell proliferation, cell adhesion, and antimicrobial activity against prokaryotic pathogens show that the nanofibers loaded with *Verbascum Thapsus* extract are effective in healing episiotomy wounds. It that this scaffold is suitable for all kinds of dressings to accelerate wound healing process and

providing a promising treatment.

Ethics approval and consent to participate

The procedures and the animal studies were performed under the ethical approval of National institute of genetic engineering and biotechnology (NIGEB) IRNIGEB.EC.1402.11.29.

Consent for publication

All the authors have approved this article and agreed with the submission.

Data availability statement

Data will be made available on request.

CRediT authorship contribution statement

Sepideh Razani: Writing – original draft, Investigation. **Mohsen Farhadpour:** Writing – original draft, Methodology, Conceptualization. **Manizheh Avatefi Hemmat:** Investigation. **Fatemeh Sadat Alamdaran:** Investigation. **Masoumeh Fakhr Taha:** Methodology. **Hossein Ali Khonakdar:** Writing – review & editing, Validation. **Matin Mahmoudifard:** Writing – review & editing, Validation, Supervision, Funding acquisition, Conceptualization.

Declaration of competing interest

There is no conflict of interest.

Acknowledgments

This study was made possible by a grant from the National Institute of Genetic Engineering and Biotechnology (NIGEB).

References

[1] F. Strodtbeck, Physiology of wound healing, Newborn Infant Nurs. Rev. 1 (1) (2001) 43–52, https://doi.org/10.1053/nbin.2001.23176.
[2] T.V.A. Lordani, et al., Therapeutic effects of medicinal plants on cutaneous wound healing in humans: a systematic review, Mediat. Inflamm. 2018 (2018), https://doi.org/10.1155/2018/7354250.
[3] O. V Salata, Applications of nanoparticles in biology and medicine, J. Nanobiotechnology 6 (3) (2004) 1–6, https://doi.org/10.1186/1477-3155-2-12.
[4] S. Subashini, K.D. Arunachalam, S.K. Annamalai, Preclinical studies on the phytochemical, antimicrobial, and wound healing properties of indigofera aspalathoides leaves, J. Pharm. Res. 4 (9) (2011) 3206–3211.
[5] R. Khan, S. Xiangyang, A. Ahmad, X. Mo, SM gr up SM journal of biomedical engineering electrospinning of crude plant extracts for antibacterial and wound healing applications : a review, SM J. Biomed. Eng. 4 (1) (2018) 1–8.
[6] B. Mehdinezhad, et al., Corresponding author comparison of in-vivo wound healing activity of verbascum thapsus flower extract with zinc oxide on experimental wound model in rabbits, Adv. Environ. Biol. 5 (7) (2011) 1501–1509.
[7] V. Prakash, S. Rana, A. Sagar, Studies on antibacterial activity of verbascum thapsus, Journal of Medicinal Plants Studies JMPS 4 (3) (2016) 101–103.
[8] M. Riaz, M. Zia-Ul-Haq, H.Z.E. Jaafar, Common mullein, pharmacological and chemical aspects, Rev. Bras. Farmacogn. 23 (6) (2013) 948–959, https://doi.org/10.1590/S0102-695X2013000600012.
[9] A.M. Khan, R.A. Qureshi, S.A. Gillani, F. Ullah, Antimicrobial activity of selected medicinal plants of Margalla hills, Islamabad, Pakistan, J. Med. Plant Res. 5 (18) (2011) 4665–4670.
[10] M. Rajbhandari, et al., Antiviral activity of some plants used in Nepalese traditional medicine, Evidence-Based Complement. Altern. Med. 6 (4) (2009) 517–522, https://doi.org/10.1093/ecam/nem156.
[11] S. Taleb, M. Saeedi, The effect of the Verbascum Thapsus on episiotomy wound healing in nulliparous women: a randomized controlled trial, BMC Complement. Med. Ther. 21 (2021) 166, https://doi.org/10.1186/s12906-021-03339-6.
[12] M. Sharifi, S.H. Bahrami, N.H. Nejad, P.B. Milan, Electrospun PCL and PLA hybrid nanofibrous scaffolds containing Nigella sativa herbal extract for effective wound healing, J. Appl. Polym. Sci. 137 (46) (2020), https://doi.org/10.1002/app.49528.
[13] M. Nasrollahzadeh, S.M. Sajadi, M. Sajjadi, Z. Issaabadi, An Introduction to Nanotechnology, first ed., vol. 28, Elsevier Ltd., 2019.
[14] N. Vahedi, F. Tabandeh, M. Mahmoudifard, Hyaluronic acid–graphene quantum dot nanocomposite: potential target drug delivery and cancer cell imaging, Biotechnol. Appl. Biochem. 69 (3) (2022) 1068–1079, https://doi.org/10.1002/bab.2178.
[15] E. Ekrami, M. Khodabandeh Shahraky, M. Mahmoudifard, M.S. Mirtaleb, P. Shariati, Biomedical applications of electrospun nanofibers in industrial world: a review, Int. J. Polym. Mater. Polym. Biomater. 72 (7) (2023) 561–575, https://doi.org/10.1080/00914037.2022.2032705.
[16] O.E. Fayemi, et al., Antimicrobial and wound healing properties of polyacrylonitrile-moringa extract nanofibers, ACS Omega 3 (5) (2018) 4791–4797, https://doi.org/10.1021/acsomega.7b01981.
[17] M. Mahmoudifard, M. Vossoughi, M. Soleimani, Different types of electrospun nanofibers and their effect on microfluidic-based immunoassay, Polym. Adv. Technol. 30 (4) (2019) 973–982, https://doi.org/10.1002/pat.4531.
[18] M. Mahmoudifard, A.M. Shoushtari, A. Mohsenifar, Fabrication and characterization study of electrospun quantum dot - poly vinyl alcohol composite nanofiber for novel engineering applications, Fibers Polym. 13 (8) (2012) 1031–1036, https://doi.org/10.1007/s12221-012-1031-x.
[19] M. Mahmoudifard, M. Vossoughi, S. Soudi, M. Soleimani, Electrospun polyethersolfone nanofibrous membrane as novel platform for protein immobilization in microfluidic systems, J. Biomed. Mater. Res. Part B Appl. Biomater. 106 (3) (2018) 1108–1120, https://doi.org/10.1002/jbm.b.33923.
[20] E. Ekrami, M. Pouresmaieli, E. sadat Hashemiyoon, N. Noorbakhsh, M. Mahmoudifard, Nanotechnology: a sustainable solution for heavy metals remediation, Environ. Nanotechnology, Monit. Manag. 18 (June) (2022) 100718, https://doi.org/10.1016/j.enmm.2022.100718.
[21] F. Barati, A.M. Farsani, M. Mahmoudifard, A promising approach toward efficient isolation of the exosomes by core–shell PCL-gelatin electrospun nanofibers, Bioprocess Biosyst. Eng. 43 (11) (2020) 1961–1971, https://doi.org/10.1007/s00449-020-02385-7.

[22] F. Barati, A. Arpanaei, M. Mahmoudifard, Highly efficient detection of cancer-derived exosomes using modified core-shell electrospun nanofibers as a capture substrate and antibody immobilized-graphene quantum dots as a signaling agent, Anal. Methods 12 (28) (2020) 3670–3681, https://doi.org/10.1039/d0ay00944j.

[23] S. Asghari, M. Mahmoudifard, Core-shell nanofibrous membrane of polycaprolactone-hyaluronic acid as a promising platform for the efficient capture and release of circulating tumor cells, Polym. Adv. Technol. 32 (3) (2021) 1101–1113, https://doi.org/10.1002/pat.5158.

[24] Z. Xie, et al., Dual growth factor releasing multi-functional nanofibers for wound healing, Acta Mater. 9 (12) (2013).

[25] K. Zhang, et al., Layered nanofiber sponge with an improved capacity for promoting blood coagulation and wound healing, Biomaterials (2019), https://doi.org/10.1016/j.biomaterials.2019.03.008.

[26] N. Charernsriwilaiwat, T. Rojanarata, T. Ngawhirunpat, M. Sukma, P. Opanasopit, Electrospun chitosan-based nanofiber mats loaded with Garcinia mangostana extracts, Int. J. Pharm. 452 (1–2) (2013) 333–343, https://doi.org/10.1016/j.ijpharm.2013.05.012.

[27] E. Zahedi, A. Esmaeili, N. Eslahi, M.A. Shokrgozar, A. Simchi, Fabrication and characterization of core-shell electrospun fibrous mats containing medicinal herbs for wound healing and skin tissue engineering, Mar. Drugs 17 (1) (2019), https://doi.org/10.3390/md17010027.

[28] F. Doustdar, S. Ramezani, M. Ghorbani, F. Mortazavi Moghadam, Optimization and characterization of a novel tea tree oil-integrated poly (ε-caprolactone)/soy protein isolate electrospun mat as a wound care system, Int. J. Pharm. 627 (September) (2022) 122218, https://doi.org/10.1016/j.ijpharm.2022.122218.

[29] E. Esmaeili, et al., The biomedical potential of cellulose acetate/polyurethane nanofibrous mats containing reduced graphene oxide/silver nanocomposites and curcumin: antimicrobial performance and cutaneous wound healing, Int. J. Biol. Macromol. 152 (2020) 418–427, https://doi.org/10.1016/j.ijbiomac.2020.02.295.

[30] M. Khalili, et al., Preparation and characterization of bi-layered polycaprolactone/polyurethane nanofibrous scaffold loaded with titanium oxide and curcumin for wound dressing applications, Appl. Phys. Mater. Sci. Process 128 (6) (2022), https://doi.org/10.1007/s00339-022-05646-2.

[31] M. Abbas, et al., Chitosan-polyvinyl alcohol membranes with improved antibacterial properties contained Calotropis procera extract as a robust wound healing agent, Arab. J. Chem. 15 (5) (2022) 103766, https://doi.org/10.1016/j.arabjc.2022.103766.

[32] B. Talib Al-Sudani, et al., Antibacterial and wound healing performance of a novel electrospun nanofibers based on polymethyl-methacrylate/gelatin impregnated with different content of propolis, J. Drug Deliv. Sci. Technol. 95 (April) (2024) 105641, https://doi.org/10.1016/j.jddst.2024.105641.

[33] P. Zhu, et al., Electrospun polylactic acid nanofiber membranes containing Capparis spinosa L. extracts for potential wound dressing applications, J. Appl. Polym. Sci. 138 (32) (2021) 1–10, https://doi.org/10.1002/app.50800.

[34] J. Yin, L. Xu, Batch preparation of electrospun polycaprolactone/chitosan/aloe vera blended nanofiber membranes for novel wound dressing, Int. J. Biol. Macromol. 160 (2020) 352–363, https://doi.org/10.1016/j.ijbiomac.2020.05.211.

[35] M. Akia, C. Rodriguez, L. Materon, R. Gilkerson, K. Lozano, Antibacterial activity of polymeric nanofiber membranes impregnated with Texas sour orange juice, Eur. Polym. J. 115 (February) (2019) 1–5, https://doi.org/10.1016/j.eurpolymj.2019.03.019.

[36] Y. Liang, et al., Adhesive hemostatic conducting injectable composite hydrogels with sustained drug release and photothermal antibacterial activity to promote full-thickness skin regeneration during wound healing, Small nano micro (2019), https://doi.org/10.1002/smll.201900046.

[37] Suvik and Effendy, The use of modified masson ' S trichrome staining in collagen evaluation in wound healing study, Malaysian Journal of Veterinary Research 3 (1) (2012) 39–47.

[38] H. Hussain, S. Aziz, G.A. Miana, V.U. Ahmad, S. Anwar, I. Ahmed, Minor chemical constituents of Verbascum thapsus, Biochem. Syst. Ecol. 37 (2) (2009) 124–126, https://doi.org/10.1016/j.bse.2008.12.007.

[39] T. Warashina, T. Miyase, A. Ueno, Phenylethanoid and lignan glycosides from Verbascum thapsus, Phytochemistry 31 (3) (1992) 961–965, https://doi.org/10.1016/0031-9422(92)80048-J.

[40] M.I. Georgiev, K. Ali, K. Alipieva, R. Verpoorte, Y.H. Choi, Metabolic differentiations and classification of Verbascum species by NMR-based metabolomics, Phytochemistry 72 (16) (2011) 2045–2051, https://doi.org/10.1016/j.phytochem.2011.07.005.

[41] M. D'Imperio, et al., Stability-activity of verbascoside, a known antioxidant compound, at different pH conditions, Food Res. Int. 66 (2014) 373–378, https://doi.org/10.1016/j.foodres.2014.09.037.

[42] V.M. Dembitsky, Astonishing diversity of natural surfactants : 5, Biologically Active Glycosides of Aromatic Metabolites 40 (9) (2005) 869–900.

[43] M. Georgiev, et al., Antioxidant activity of devil's claw cell biomass and its active constituents, Food Chem. 121 (4) (2010) 967–972, https://doi.org/10.1016/j.foodchem.2010.01.028.

[44] A.M. Díaz, M.J. Abad, L. Fernández, A.M. Silván, J. De Santos, P. Bermejo, Phenylpropanoid glycosides from Scrophularia scorodonia: in vitro anti-inflammatory activity, Life Sci. 74 (20) (2004) 2515–2526, https://doi.org/10.1016/j.lfs.2003.10.008.

[45] Z. Akdemir, Ç. Kahraman, I.I. Tatli, E. Küpeli Akkol, I. Süntar, H. Keles, Bioassay-guided isolation of anti-inflammatory, antinociceptive and wound healer glycosides from the flowers of Verbascum mucronatum Lam, J. Ethnopharmacol. 136 (3) (2011) 436–443, https://doi.org/10.1016/j.jep.2010.05.059.

[46] V. Mihailović, S. Kreft, E.T. Benković, N. Ivanović, M.S. Stanković, Chemical profile, antioxidant activity and stability in stimulated gastrointestinal tract model system of three Verbascum species, Ind. Crops Prod. 89 (2016) 141–151, https://doi.org/10.1016/j.indcrop.2016.04.075.

[47] K.M. Soto, et al., Gold nanoparticles synthesized with common mullein (verbascum thapsus) and Castor bean (Ricinus communis) ethanolic extracts displayed antiproliferative effects and induced caspase 3 activity in human HT29 and SW480 cancer cells, Pharmaceutics 14 (10) (2022), https://doi.org/10.3390/pharmaceutics14102069.

[48] L.R. Aldaba-muruato, et al., Therapeutic perspectives of p-coumaric acid: anti-necrotic, anti-cholestatic and anti-amoebic activities, World Acad. Sci. J. 3 (5) (2021) 1–8, https://doi.org/10.3892/wasj.2021.118.

[49] A.A. Amer, R.S. Mohammed, Y. Hussein, A.S.M. Ali, A.A. Khalil, Development of lepidium sativum extracts/PVA electrospun nanofibers as wound healing dressing, ACS Omega 7 (24) (2022) 20683–20695, https://doi.org/10.1021/acsomega.2c00912.

[50] A. Haider, S. Haider, I.K. Kang, A comprehensive review summarizing the effect of electrospinning parameters and potential applications of nanofibers in biomedical and biotechnology, Arab. J. Chem. 11 (8) (2018) 1165–1188, https://doi.org/10.1016/j.arabjc.2015.11.015.

[51] A. Fahami, M. Fathi, Development of cress seed mucilage/PVA nanofibers as a novel carrier for vitamin A delivery, Food Hydrocoll 81 (2018) 31–38, https://doi.org/10.1016/j.foodhyd.2018.02.008.

[52] N. Okutan, P. Terzi, F. Altay, Affecting parameters on electrospinning process and characterization of electrospun gelatin nanofibers, Food Hydrocoll 39 (2014) 19–26, https://doi.org/10.1016/j.foodhyd.2013.12.022.

[53] M. Hashmi, S. Ullah, I.S. Kim, Electrospun Momordica charantia incorporated polyvinyl alcohol (PVA) nanofibers for antibacterial applications, Mater. Today Commun. 24 (2020) 101161, https://doi.org/10.1016/j.mtcomm.2020.101161.

[54] M. Hulupi, H. Haryadi, Synthesis and characterization of electrospinning PVA nanofiber-crosslinked by glutaraldehyde, Mater. Today Proc. 13 (2019) 199–204, https://doi.org/10.1016/j.matpr.2019.03.214.

[55] H.S. Mansur, C.M. Sadahira, A.N. Souza, A.A.P. Mansur, FTIR spectroscopy characterization of poly (vinyl alcohol) hydrogel with different hydrolysis degree and chemically crosslinked with glutaraldehyde, Mater. Sci. Eng. 28 (2007) 539–548, https://doi.org/10.1016/j.msec.2007.10.088.

[56] S.R. Sudhamani, M.S. Prasad, K.U. Sankar, DSC and FTIR studies on Gellan and Polyvinyl alcohol (PVA) blend films, Food Hydrocolloid 17 (2002) 245–250, https://doi.org/10.1016/S0268-005X(02)00057-7.

[57] H.S. Mansur, R.L. Oréfice, A.A.P. Mansur, Characterization of poly(vinyl alcohol)/poly(ethylene glycol) hydrogels and PVA-derived hybrids by small-angle X-ray scattering and FTIR spectroscopy, Polymer (Guildf). 45 (21) (2004) 7193–7202, https://doi.org/10.1016/j.polymer.2004.08.036.

[58] M. Saleh, H. Arslan, Z. Isik, M. Yalvac, N. Dizge, The use of verbascum thapsus L as a biomembrane for activated sludge filtration, Avicenna J Env. Heal. 8 (2) (2021) 102–109, https://doi.org/10.34172/ajehe.2021.13.

[59] L. Marion, D.A. Ramsay, R. Norman Jones, The infrared absorption spectra of alkaloids, J. Am. Chem. Soc. 73 (1) (1951) 305–308, https://doi.org/10.1021/ja01145a100.

[60] G. Ajmal, G.V. Bonde, P. Mittal, G. Khan, V.K. Pandey, B.V. Bakade, B. Mishra, Biomimetic PCL-gelatin based nanofibers loaded with ciprofloxacin hydrochloride and quercetin: a potential antibacterial and anti-oxidant dressing material for accelerated healing of a full thickness wound, Int. J. Pharm. 567 (2019), https://doi.org/10.1016/j.ijpharm.2019.118480.
[61] Hassan Maleki, et al., Zingiber officinale and thymus vulgaris extracts co-loaded polyvinyl alcohol and chitosan electrospun nanofibers for tackling infection and wound healing promotion, Heliyon 10 (1) (2024) e23719. .
[62] S.M. Patil, R. Ramu, P.S. Shirahatti, C. Shivamallu, R.G. Amachawadi, A systematic review on ethnopharmacology, phytochemistry and pharmacological aspects of Thymus vulgaris Linn, Heliyon 7 (2021) e07054, https://doi.org/10.1016/j.heliyon.2021.e07054.
[63] M.P. Mani, S.K. Jaganathan, A.F. Ismail, Appraisal of electrospun textile scaffold comprising polyurethane decorated with ginger nanofibers for wound healing applications, J. Ind. Text. 49 (5) (2019) 648–662, https://doi.org/10.1177/1528083718795911.
[64] M. Khalili, et al., Preparation and characterization of nanofibrous scaffolds containing copper nanoparticles and curcumin for wound healing applications, Polym. Bull. (2024) 0123456789, https://doi.org/10.1007/s00289-024-05148-6.
[65] M.M. Gonçalves, et al., Preparation and characterization of a novel antimicrobial film dressing for wound healing application, Brazilian J. Pharm. Sci. 56 (2020) 1–11, https://doi.org/10.1590/S2175-97902020000118784.
[66] P. Wu, A.C. Fisher, P.P. Foo, D. Queen, J.D.S. Gaylor, In vitro assessment of water vapour transmission of synthetic wound dressings, Biomaterials 16 (3) (1995) 171–175, https://doi.org/10.1016/0142-9612(95)92114-L.
[67] L.A. Smith, P.X. Ma, Nano-fibrous scaffolds for tissue engineering, Colloids Surfaces B Biointerfaces 39 (3) (2004) 125–131, https://doi.org/10.1016/j.colsurfb.2003.12.004.
[68] P. Karuppuswamy, J.R. Venugopal, B. Navaneethan, A.L. Laiva, S. Sridhar, S. Ramakrishna, Functionalized hybrid nanofibers to mimic native ECM for tissue engineering applications, Appl. Surf. Sci. 322 (2014) 162–168, https://doi.org/10.1016/j.apsusc.2014.10.074.
[69] A. Chanda, et al., Electrospun chitosan/polycaprolactone-hyaluronic acid bilayered scaffold for potential wound healing applications, Int. J. Biol. Macromol. 116 (2017) (2018) 774–785, https://doi.org/10.1016/j.ijbiomac.2018.05.099.
[70] A. Jafari, A. Amirsadeghi, S. Hassanajili, N. Azarpira, Bioactive antibacterial bilayer PCL/gelatin nanofibrous scaffold promotes full-thickness wound healing, Int. J. Pharm. 583 (May) (2020) 119413, https://doi.org/10.1016/j.ijpharm.2020.119413.
[71] S. Ravichandran, J. Radhakrishnan, P. Jayabal, G.D. Venkatasubbu, Antibacterial Screening Studies of Electrospun Polycaprolactone Nano Fibrous Mat Containing Clerodendrum Phlomidis Leaves Extract, vol. 484, Elsevier B.V, 2019.
[72] A.U. Turker, N.D. Camper, Biological activity of common mullein, a medicinal plant, J. Ethnopharmacol. 82 (2–3) (2002) 117–125, https://doi.org/10.1016/S0378-8741(02)00186-1.
[73] K. Nofouzi, R. Mahmudi, K. Tahapour, E. Amini, K. Yousefi, Verbascum speciosum methanolic extract: phytochemical components and antibacterial properties, J. Essent. Oil-Bearing Plants 19 (2) (2016) 499–505, https://doi.org/10.1080/0972060X.2014.901625.
[74] E. Röder, Medicinal plants in Europe containing pyrrolizidine alkaloids, Pharmazie 50 (2) (1995) 83–98.
[75] O.C. Seremet, et al., Toxicity of plant extracts containing pyrrolizidine alkaloids using alternative invertebrate models, Mol. Med. Rep. 17 (6) (2018) 7757–7763, https://doi.org/10.3892/mmr.2018.8795.
[76] I.I. Tatli, Akdemir, and Zeliha, "chemical cons. of verbascum L.species,", J. Pharm. Sci 29 (2004) 93–107 [Online]. Available, http://www.fabad.org.tr/eski/fabad.org/pdf/volum29/issue2/FABAD2004j.Pharm.Sci.,29,93-107,2004.pdf.
[77] G.M. Rukunga, P.G. Waterman, New macrocyclic spermine (budmunchiamine) alkaloids from Albizia gummifera: with some observations on the structure-activity relationships of the budmunchiamines, Journal of Natural Products 59 (9) (1996) 850–853, https://doi.org/10.1021/np960397d.
[78] G.G. Leitão, C.M. Leal, S.C. Mendonça, R. Pereda-Miranda, Ification of alkaloids by countercurrent chromatography, Soc. Bras. Farmacogn. (2021), https://doi.org/10.1007/s43450-021-00163-4.
[79] M. Bagheri, M. Validi, A. Gholipour, P. Makvandi, E. Sharifi, Chitosan nanofiber biocomposites for potential wound healing applications: antioxidant activity with synergic antibacterial effect, Bioeng. Transl. Med. 7 (1) (2022) 1–15, https://doi.org/10.1002/btm2.10254.
[80] K. Murti, V. Lambole, M. Panchal, Effect of Ficus hispida L. on normal and dexamethasone suppressed wound healing, Brazilian J. Pharm. Sci. 47 (4) (2011) 855–860, https://doi.org/10.1590/S1984-82502011000400023.
[81] H.R. Kavousi, M.R. Karimi, M.G. Neghab, Assessment the copper-induced changes in antioxidant defense mechanisms and copper phytoremediation potential of common mullein (Verbascum thapsus L.), Environ. Sci. Pollut. Res. 28 (14) (2021) 18070–18080, https://doi.org/10.1007/s11356-020-11903-9.
[82] I. Süntar, I.I. Tatli, E. Küpeli Akkol, H. Keleş, Ç. Kahraman, Z. Akdemir, An ethnopharmacological study on Verbascum species: from conventional wound healing use to scientific verification, J. Ethnopharmacol. 132 (2) (2010) 408–413, https://doi.org/10.1016/j.jep.2010.08.004.
[83] S. Gonca, H. Arslan, Z. Isik, S. Özdemirc, N. Dizge, The surface modification of ultrafiltration membrane with silver nanoparticles using Verbascum thapsus leaf extract using green synthesis phenomena, Surface. Interfac. (2021), https://doi.org/10.1016/j.surfin.2021.101291.
[84] F. Reesi, M. Minaiyan, A. Taheri, A novel lignin-based nanofibrous dressing containing arginine for wound-healing applications, Drug Deliv. Transl. Res. 8 (1) (2018) 111–122, https://doi.org/10.1007/s13346-017-0441-0.
[85] R. Ramalingam, et al., Core-Shell structured antimicrobial nanofiber dressings containing herbal extract and antibiotics combination for the prevention of biofilms and promotion of cutaneous wound healing, ACS Appl. Mater. Interfaces (2021), https://doi.org/10.1021/acsami.0c20642.
[86] B. Motealleh, P. Zahedi, I. Rezaeian, M. Moghimi, A.H. Abdolghaffari, M.A. Zarandi, Morphology, drug release, antibacterial, cell proliferation, and histology studies of chamomile-loaded wound dressing mats based on electrospun nanofibrous poly(ε-caprolactone)/polystyrene blends, J. Biomed. Mater. Res. Part B Appl. Biomater. 102 (5) (2014) 977–987, https://doi.org/10.1002/jbm.b.33078.
[87] A.C.D.O. Gonzalez, Z.D.A. Andrade, T.F. Costa, A.R.A.P. Medrado, Wound healing - a literature review, An. Bras. Dermatol. 91 (5) (2016) 614–620, https://doi.org/10.1590/abd1806-4841.20164741.
[88] V. Alexandru, A. Gaspar, S. Savin, A. Toma, R. Tatia, E. Gille, Phenolic content, antioxidant activity and effect on collagen synthesis of a traditional wound healing polyherbal formula, Stud. Univ. Vasile Goldis Arad, Ser. Stiint. Vietii 25 (1) (2015) 41–46.
[89] B.P. Antunes, A.F. Moreira, V.M. Gaspar, I.J. Correia, Chitosan/arginine-chitosan polymer blends for assembly of nanofibrous membranes for wound regeneration, Carbohydr. Polym. 130 (2015) 104–112, https://doi.org/10.1016/j.carbpol.2015.04.072.
[90] S. Ellis, E.J. Lin, D. Tartar, Immunology of wound healing, Curr. Dermatol. Rep. 7 (4) (2018) 350–358, https://doi.org/10.1007/s13671-018-0234-9.
[91] C. Qing, The molecular biology in wound healing & non-healing wound, Chinese J. Traumatol. - English Ed. 20 (4) (2017) 189–193, https://doi.org/10.1016/j.cjtee.2017.06.001.